

# A Primal-Dual-Based Active Fault-Tolerant Control Scheme for Cyber-Physical Systems: Application to DC Microgrids

Wasif H. Syed\*, Juan E. Machado\*, Johannes Schiffer\*<sup>§</sup>

\* *Chair of Control Systems and Network Control Technology,  
Brandenburg University of Technology Cottbus–Senftenberg,  
Cottbus, Germany,*

{syed,machadom,schiffer}@b-tu.de.

<sup>§</sup> *Fraunhofer Institute for Energy Infrastructures and Geotechnologies,  
Cottbus, Germany.*

## Abstract

We consider the problem of active fault-tolerant control in cyber-physical systems composed of strictly passive linear-time invariant dynamic subsystems. We cast the problem as a constrained optimization problem and propose an augmented primal-dual gradient dynamics-based fault-tolerant control framework that enforces network-level constraints and provides optimality guarantees for the post-fault steady-state operation. By suitably interconnecting the primal-dual algorithm with the cyber-physical dynamics, we provide sufficient conditions under which the resulting closed-loop system possesses a unique and exponentially stable equilibrium point that satisfies the Karush–Kuhn–Tucker (KKT) conditions of the constrained problem. The framework’s effectiveness is illustrated through numerical experiments on a DC microgrid.

## Index Terms

Fault-Tolerant Control, Primal-Dual Dynamics, Distributed Control, Microgrids, Constraint Optimization, Optimal Control.

## I. INTRODUCTION

A cyber-physical system (CPS) consists of several subsystems coupled through a physical infrastructure and a flexible communication layer [1]. Such architectures are now widespread in industrial automation (e.g., smart grids, manufacturing, process control, automotive systems, and intelligent highways), motivating extensive research on their modeling, analysis, and control [2]. In many classes of CPSs the subsystems must act cooperatively, for instance power plants jointly meeting a city’s demand, trucks platooning, or tugboats coordinating maneuvers in ports [1]. However, conventional feedback control can lead to underperformance or even instability under component malfunctions, which is particularly undesired in safety-critical applications [3]. This motivates the development of fault-tolerant control (FTC) schemes that maintain acceptable performance despite faults and other abrupt changes in CPS dynamics [4].

FTC schemes are commonly categorized into passive or active approaches [4]. On the one hand, passive FTC would typically employ a fixed robust controller to tolerate anticipated faults without reconfiguration. However, its effectiveness can degrade under large or multiple faults. On the other hand, active FTC typically entails a controller reconfiguration (or of its parameters) after fault detection (and isolation) in order to recover acceptable performance [4]. In this paper, we focus on active FTC design for a class of CPSs in which each subsystem has strictly passive dynamics and in which subsystem interconnections are power-preserving, leading to an overall CPS which remains strictly passive, thereby providing a structured basis for FTC design<sup>1</sup>.

Active FTC design has been explored in [1], [7]–[9] from the viewpoint of flexible task assignment: when a subsystem is degraded, the cooperative objective is redistributed according to residual capabilities, leveraging system-level redundancy without reconfiguring local controllers. Moreover, a decentralized adaptive FTC scheme based on backstepping is studied in [10], where each subsystem is rendered input-to-state stable with respect to its interconnection inputs and cyclic small-gain conditions are enforced, ensuring network-level stability under actuator faults and disturbances. In [4], a distributed tube-based MPC is used for active fault isolation/diagnosis in CPS: diagnostic inputs are optimized to separate fault models while constraints are enforced locally via invariant tubes; if reconfiguration is infeasible, the affected subsystem is unplugged.

This work is partially supported by the Bundesministerium für Wirtschaft und Klimaschutz (BMWK), Germany under LuFo VI - 2 joint project “Safe and reliable electrical and thermal networks for hybrid-electric drive systems (ETHAN, project number: 20L2103F1”. This research is also supported by the German Federal Government, the Federal Ministry of Research, Technology and Space (BMFTR) and the State of Brandenburg within the framework of the joint project EIZ: Energy Innovation Center (project numbers 85056897 and 03SF0693A) with funds from the Structural Development Act (Strukturstärkungsgesetz) for coal-mining regions.

<sup>1</sup>In many CPSs, subsystems are passive either due to inherent physical properties [5] or can be rendered passive via local control [6].

Overall, the above-mentioned FTC design approaches provide valuable mechanisms for fault accommodation (task redistribution, adaptive compensation, or diagnosis). However, they lack a network-level constrained optimization with explicit optimality guarantees that co-optimizes post-fault performance under coupled constraints (e.g., shared resources and interconnection limits), which is central in CPSs such as power and energy networks (e.g., microgrids). To address these limitations, in the present work we make the following contributions to FTC design for (strictly passive) CPSs:

- We cast the post-fault network operation of a CPS as a constrained convex optimization problem and formulate an augmented primal-dual gradient dynamics (Aug-PDGD) for its solution. The Aug-PDGD enables strict constraint satisfaction, and exhibits an energy-/cost-optimal operating point.
- By suitably interconnecting the considered strictly passive CPS with the Aug-PDGD, we provide an explicit characterization of the controller parameters under which the resulting closed-loop system admits an exponentially stable equilibrium point that satisfies the Karush–Kuhn–Tucker (KKT) conditions of the constrained problem. This is accomplished by combining prior results in [11] that establish exponential stability of the equilibrium of the Aug-PDGD with the control-by-interconnection (CBI) framework [12].
- We demonstrate the potential of the proposed FTC for CPSs via an application to class of clustered DC microgrids. This is particularly appealing scenario, since following a capacity degradation or outage, the FTC based on the Aug-PDGD computes the least-cost, loss-aware redistribution of generation while respecting practical limits on voltages and currents.

#### Notation

The notation used in this paper is as follows. For elements  $x_i \in \mathbb{R}$ , the expression  $x = \text{col}(x_i)$  denotes the column vector formed by stacking  $x_i$ . The operators  $\text{diag}(x_i)$  and  $\text{blkdiag}(x_i)$  denote diagonal and block-diagonal matrices with entries or blocks  $x_i$ , respectively. The symbols  $\mathbf{I}$  and  $\mathbf{0}$  denote the identity and zero matrices of appropriate dimensions. For any signal  $x : \mathbb{R} \rightarrow \mathbb{R}^n$ , the deviation from a constant  $\bar{x} \in \mathbb{R}^n$  is written as  $\tilde{x} = x - \bar{x}$ . For any symmetric matrix  $M \in \mathbb{R}^{n \times n}$ , the quadratic form  $x^\top M x$  is compactly written as  $\|x\|_M^2$ . For two symmetric matrices  $A$  and  $B$ , the notation  $A \succ B$  (respectively  $A \succeq B$ ) means that  $A - B$  is positive definite (respectively positive semidefinite). For a square matrix  $M$ ,  $\lambda_i(M)$  denotes its  $i$ -th eigenvalue, and  $\text{Re}(\lambda_i(M))$  denotes its real part. The symbol  $\lambda_{\max}(M)$  denotes the largest eigenvalue of a symmetric matrix  $M$ . For any collection of matrices  $M_{i,j}$ , the notation  $[M_{i,j}]_{i,j=1}^N$  denotes the block matrix obtained by placing  $M_{i,j}$  in the  $(i,j)$ -th block position. For any set  $S \subset \mathbb{R}^n$ ,  $\text{conv}(S)$  denotes its convex hull.

## II. CPS MODEL

### A. Subsystem dynamics and interconnection rule

We consider a CPS composed of  $N > 1$  interconnected LTI subsystems with dynamics

$$\dot{x}_i = A_i x_i + B_i u_i + d_i + G_i w_i, \quad (1a)$$

$$y_i = C_i x_i, \quad (1b)$$

$$z_i = E_i x_i, \quad (1c)$$

where  $x_i \in \mathbb{R}^{n_i}$  is the state,  $u_i \in \mathbb{R}^{m_i}$  is the control input,  $y_i \in \mathbb{R}^{p_i}$  is the measured output,  $z_i \in \mathbb{R}^{s_i}$  is the interconnection output,  $w_i \in \mathbb{R}^{q_i}$  is the interconnection input, and  $d_i \in \mathbb{R}^{n_i}$  is a constant vector,  $i = 1, \dots, N$ . The interconnection of the  $i$ -th subsystem with other subsystems is given by

$$w_i = \sum_{j=1}^N \Omega_{i,j} z_j, \quad (2)$$

with constant matrices  $\Omega_{i,j} \in \mathbb{R}^{q_i \times s_j}$ , which are only nonzero if subsystem  $i$  is connected to subsystem  $j$  via a physical link.

We make the following technical assumptions on the dynamics (1), (2),  $i = 1, \dots, N$ .

*Assumption 1:* For each  $i = 1, \dots, N$ , the triples  $(A_i, B_i, C_i)$  and  $(A_i, G_i, E_i)$  in (1) are minimal, and the transfer function matrices

$$G_{p,i}(s) = C_i(s\mathbf{I} - A_i)^{-1} B_i \quad \text{and} \quad G_{z,i}(s) = E_i(s\mathbf{I} - A_i)^{-1} G_i$$

are strictly positive real (SPR), where  $s \in \mathbb{C}$  is the Laplace variable. □

*Assumption 2:* The interconnection (2) of any two subsystems (1) is power-preserving, i.e.,

$$\Omega_{i,j} + \Omega_{j,i}^\top = \mathbf{0} \quad \forall i = 1, \dots, N, \quad \forall j = 1, \dots, N, \quad j \neq i. \quad \square$$

Assumption 1 ensures that each subsystem is internally stable, i.e.,  $A_i$  is Hurwitz, and strictly passive in the input–output pairs  $(u_i, y_i)$  and  $(w_i, z_i)$  [13]<sup>2</sup>. Assumption 2 guarantees that the coupling does not inject energy into the network and

<sup>2</sup>In practice, this may result from intrinsic plant properties or from a local pre-stabilizing controller, in which case  $u_i$  acts as a supervisory input to achieve objectives other than stability.

preserves passivity when subsystems are interconnected [5].

### B. Compact CPS model

Considering (1) and (2), for  $i = 1, \dots, N$ , let  $x = \text{col}(x_1, \dots, x_N) \in \mathbb{R}^n$ ,  $u = \text{col}(u_1, \dots, u_N) \in \mathbb{R}^m$ ,  $y = \text{col}(y_1, \dots, y_N) \in \mathbb{R}^p$ ,  $z = \text{col}(z_1, \dots, z_N) \in \mathbb{R}^s$ , and  $d = \text{col}(d_1, \dots, d_N) \in \mathbb{R}^n$ . Moreover, let  $A = \text{blkdiag}(A_i)$ ,  $B = \text{blkdiag}(B_i)$ ,  $C = \text{blkdiag}(C_i)$ ,  $E = \text{blkdiag}(E_i)$ ,  $G = \text{blkdiag}(G_i)$ , and  $\Omega = [\Omega_{i,j}]_{i,j=1}^N$ . By noting that  $w = \Omega z$  and  $z = Ex$ , then the overall CPS model (1), (2),  $i = 1, \dots, N$ , can be written compactly as

$$\Sigma_P : \begin{cases} \dot{x} = Ax + Bu + d + G\Omega Ex, \\ y = Cx, \\ z = Ex. \end{cases} \quad (3)$$

We make the following assumption on the existence of a desired equilibrium point of the uncontrolled CPS (3).

*Assumption 3:* With  $u = u_i^* = \mathbf{0}$ , the interconnected system (3) admits an exponentially stable equilibrium point  $x^*$  with output  $y^*$ . At equilibrium, each subsystem satisfies the constraints  $x_i^* \in \mathcal{X}_i$ ,  $y_i^* \in \mathcal{Y}_i$  and  $u_i^* \in \mathcal{U}_i$ , where

$$\mathcal{X}_i = \{x_i \in \mathbb{R}^{n_i} \mid R_{\text{eq},x,i}x_i = b_{x,i}, R_{\text{ineq},x,i}x_i \leq h_{x,i}\}, \quad (4a)$$

$$\mathcal{Y}_i = \{y_i \in \mathbb{R}^{p_i} \mid R_{\text{eq},y,i}y_i = b_{y,i}, R_{\text{ineq},y,i}y_i \leq h_{y,i}\}, \quad (4b)$$

$$\mathcal{U}_i = \{u_i \in \mathbb{R}^{m_i} \mid R_{\text{eq},u,i}u_i = b_{u,i}, R_{\text{ineq},u,i}u_i \leq h_{u,i}\} \quad (4c)$$

are convex sets<sup>3</sup>.  $\square$

The following lemma states that the CPS model (3) is strictly shifted-passive. This property is actively exploited for the subsequent FTC design and corresponding closed-loop stability analysis.

*Lemma 1:* Fix  $0 < \tau_1 < 2 \min_i \{-\text{Re}(\lambda_i(A_p))\}$ . With  $A_p = A + G\Omega E$ , there is a unique solution  $P_1 \succ 0$  to the Lyapunov equation

$$A_p^\top P_1 + P_1 A_p = -\tau_1 P_1, \quad (5)$$

and the plant dynamics (3) are strictly shifted-passive with quadratic storage function  $S_p(\tilde{x}) = \frac{1}{2}\|\tilde{x}\|_{P_1}^2$  and with respect to the input–output pair  $(\tilde{u}, \tilde{y})$ . In particular, it holds that

$$\dot{S}_p(\tilde{x}) = -\tau_1 \tilde{x}^\top P_1 \tilde{x} + \tilde{y}^\top \tilde{u}, \quad (6)$$

along any system trajectory.  $\square$

**Proof.** Assumptions 1 and 2 imply that  $\Sigma_P$  in (3) is a power-preserving interconnection of SPR subsystems. Then, the transfer function matrix  $G_p(s)$  of the error dynamics, given by

$$G_p(s) = C(s\mathbf{I} - A_p)^{-1}B,$$

is SPR. This implies in particular that  $A_p$  is Hurwitz (see [13, Lemmas 6.3 and 6.4]). Then there exists a unique matrix  $P_1 = P_1^\top > 0$  that solves (5). It is straightforward to verify that, along system trajectories, the time-derivative of the storage function  $S_p$  satisfies (6).  $\blacksquare$

## III. PROBLEM STATEMENT AND SOLUTION APPROACH

### A. Problem Statement

Assume that at time  $t_f$ , the subsystem  $i_f$  experiences a fault (e.g., actuator failure or an additive disturbance), leading to the reconfigured dynamics of (1), (2), for the  $i_f$ -th subsystem:

$$\dot{\hat{x}}_{i_f} = \hat{A}_{i_f} \hat{x}_{i_f} + \hat{B}_{i_f} \hat{u}_{i_f} + \hat{d}_{i_f} + \hat{G}_{i_f} \hat{w}_{i_f}, \quad (7a)$$

$$\hat{y}_{i_f} = \hat{C}_{i_f} \hat{x}_{i_f}, \quad (7b)$$

$$\hat{z}_{i_f} = \hat{E}_{i_f} \hat{x}_{i_f}, \quad (7c)$$

with interconnection

$$\hat{w}_{i_f} = \hat{\Omega}_{i_f, i_f} \hat{z}_{i_f} + \sum_{j \neq i_f} \hat{\Omega}_{i_f, j} z_j,$$

<sup>3</sup> $R_{\text{eq},x,i} \in \mathbb{R}^{r_{x,i} \times n_i}$ ,  $b_{x,i} \in \mathbb{R}^{r_{x,i}}$ ,  $R_{\text{ineq},x,i} \in \mathbb{R}^{k_{x,i} \times n_i}$ ,  $h_{x,i} \in \mathbb{R}^{k_{x,i}}$ ,  $R_{\text{eq},y,i} \in \mathbb{R}^{r_{y,i} \times p_i}$ ,  $b_{y,i} \in \mathbb{R}^{r_{y,i}}$ ,  $R_{\text{ineq},y,i} \in \mathbb{R}^{k_{y,i} \times p_i}$ ,  $h_{y,i} \in \mathbb{R}^{k_{y,i}}$ ,  $R_{\text{eq},u,i} \in \mathbb{R}^{r_{u,i} \times m_i}$ ,  $b_{u,i} \in \mathbb{R}^{r_{u,i}}$ ,  $R_{\text{ineq},u,i} \in \mathbb{R}^{k_{u,i} \times m_i}$ ,  $h_{u,i} \in \mathbb{R}^{k_{u,i}}$  are user-defined constraint parameters.

and with all variables and matrices defined analogously to (1)<sup>4</sup>. We assume that Assumptions 1 and 2 remain valid for the faulty subsystem (7). Moreover, we consider that a fault may produce either one, or a combination, of the following situations:

- **Steady-state error:**  $\bar{x}_i \neq x_i^*$  or  $\bar{\hat{x}}_{i_f} \neq \hat{x}_{i_f}^*$ .
- **Output error:**  $\bar{y}_i \neq y_i^*$  or  $\hat{y}_{i_f} \neq \hat{y}_{i_f}^*$ .
- **Constraint violation:**  $\bar{x}_i \notin \mathcal{X}_i$ ,  $\bar{\hat{x}}_{i_f} \notin \hat{\mathcal{X}}_{i_f}$ ,  $\bar{y}_i \notin \mathcal{Y}_i$ ,  $\bar{\hat{y}}_{i_f} \notin \hat{\mathcal{Y}}_{i_f}$ <sup>5</sup>.

Then, the problem we address in this paper is that of designing a dynamic, feedback control law for the control input  $u$  that computes a new feasible operating point that minimizes the error with respect to the pre-fault equilibrium—while satisfying all post-fault physical and operational constraints—and that renders such an optimal equilibrium exponentially stable. Formally, let  $J : \mathbb{R}^n \times \mathbb{R}^p \times \mathbb{R}^m \rightarrow \mathbb{R}$ , denote a cost function penalizing the error between a post-fault equilibrium triple  $(\bar{x}, \bar{y}, \bar{u})$  and the pre-fault desired equilibrium  $(x^*, y^*, u^*)$ . Then our goal is to design a FTC scheme consisting of a continuous controller for  $u = \text{col}(u_i)$ , such that the CPS trajectories remain bounded and  $x \rightarrow \bar{x} = \text{col}(\bar{x}_i)$ , exponentially fast, as  $t \rightarrow \infty$ , where  $\bar{x}$  is the solution of the following steady-state optimization problem:

$$\begin{aligned} & \min_{\bar{x}, \bar{y}, \bar{u}} J(\bar{x}, \bar{y}, \bar{u}) \\ \text{s.t. } & 0 = (A + G\Omega E)\bar{x} + B\bar{u} + d, \\ & \bar{y} = C\bar{x}, \\ & \bar{x} \in \mathcal{X}, \bar{y} \in \mathcal{Y}, \bar{u} \in \mathcal{U}, \end{aligned} \tag{8}$$

where  $\mathcal{X} = \prod_{i=1}^N \mathcal{X}_i$ ,  $\mathcal{Y} = \prod_{i=1}^N \mathcal{Y}_i$ , and  $\mathcal{U} = \prod_{i=1}^N \mathcal{U}_i$ , with  $\mathcal{X}_i$ ,  $\mathcal{Y}_i$  and  $\mathcal{U}_i$  defined in (4). A simple choice for  $J$  is a quadratic function of the form

$$J(\bar{x}, \bar{y}, \bar{u}) = \frac{1}{2} \|\bar{x} - x^*\|_{K_x}^2 + \frac{1}{2} \|\bar{y} - y^*\|_{K_y}^2 + \frac{1}{2} \|\bar{u} - u^*\|_{K_u}^2,$$

with  $K_x \succ 0$ ,  $K_y \succ 0$ , and  $K_u \succ 0$ . Nonetheless, in our analysis other type of cost functions can be considered as long as they satisfy a strong convexity assumption (see Assumption 4 in Section IV for details.)

### B. Solution Approach

Following [14], [15], the approach we employ to solve the considered control problem consists in formulating a continuous-time Aug-PDGD associated to (8), and, after fitting it with suitable input channels, use it as a dynamic feedback controller in a CbI [12] fashion. Unlike [14], [15], we employ the augmented version rather than the standard PDGD, leveraging the theoretical and numerical benefits discussed in [11]. Moreover, the considered CbI-based design differs from the time-scale separation approach in [16] in the sense that our scheme actively exploits both the plant's and the augmented PDGD's strict shifted-passivity properties, which enables the explicit construction of a Lyapunov function for establishing exponential stability of the closed-loop system equilibrium<sup>6</sup>.

## IV. PROPOSED ACTIVE PRIMAL-DUAL FTC SCHEME

### A. Derivation of the Aug-PDGD

For deriving the Aug-PDGD, we begin by reformulating the optimization problem (8) as follows:

$$\begin{aligned} & \min_{\bar{\xi}} J(\bar{\xi}) \\ \text{subject to } & R_{\text{eq}} \bar{\xi} = b, \\ & R_{\text{ineq}} \bar{\xi} \leq h, \end{aligned} \tag{9a}$$

where

$$\bar{\xi} = \text{col}(\bar{x}, \bar{y}, \bar{u}) \in \mathbb{R}^{n_{\xi} = n + p + m}, \tag{9b}$$

<sup>4</sup>In particular,  $\hat{x}_{i_f} \in \mathbb{R}^{n_{i_f}}$ ,  $\hat{u}_{i_f} \in \mathbb{R}^{m_{i_f}}$ ,  $\hat{y}_{i_f} \in \mathbb{R}^{p_{i_f}}$ ,  $\hat{z}_{i_f} \in \mathbb{R}^{s_{i_f}}$ ,  $\hat{w}_{i_f} \in \mathbb{R}^{q_{i_f}}$ ,  $\hat{d}_{i_f} \in \mathbb{R}^{n_{i_f}}$ ,  $\hat{A}_{i_f} \in \mathbb{R}^{n_{i_f} \times n_{i_f}}$ ,  $\hat{B}_{i_f} \in \mathbb{R}^{n_{i_f} \times m_{i_f}}$ ,  $\hat{G}_{i_f} \in \mathbb{R}^{n_{i_f} \times q_{i_f}}$ ,  $\hat{C}_{i_f} \in \mathbb{R}^{p_{i_f} \times n_{i_f}}$ ,  $\hat{E}_{i_f} \in \mathbb{R}^{s_{i_f} \times n_{i_f}}$ ,  $\hat{\Omega}_{i_f, j} \in \mathbb{R}^{q_{i_f} \times s_j}$ .

<sup>5</sup>To simplify the notation, we henceforth drop the use of the symbol  $(\cdot)$  for the faulty subsystem (7).

<sup>6</sup>Other benefits of using a dynamic controller based on the Aug-PDGD, instead of using a static feedforward input  $u = \bar{u}$  that solves (4), is that it yields a feedback-optimization architecture that adapts online, improving robustness and performance and enabling real-time adjustment of  $\bar{u}$  under disturbances [17].

$$R_{\text{eq}} = \begin{bmatrix} -C & \mathbf{I} & \mathbf{0} \\ A + G\Omega E & \mathbf{0} & B \\ R_{\text{eq},x} & \mathbf{0} & \mathbf{0} \\ \mathbf{0} & R_{\text{eq},y} & \mathbf{0} \\ \mathbf{0} & \mathbf{0} & R_{\text{eq},u} \end{bmatrix} \in \mathbb{R}^{n_{\text{eq}} \times n_{\xi}}, \quad (9c)$$

$$R_{\text{ineq}} = \begin{bmatrix} R_{\text{ineq},x} & \mathbf{0} & \mathbf{0} \\ \mathbf{0} & R_{\text{ineq},y} & \mathbf{0} \\ \mathbf{0} & \mathbf{0} & R_{\text{ineq},u} \end{bmatrix} \in \mathbb{R}^{n_{\text{ineq}} \times n_{\xi}}, \quad (9d)$$

$$b := \text{col}(\mathbf{0}, -d, b_x, b_y, b_u) \in \mathbb{R}^{n_{\text{eq}}}, \quad (9e)$$

$$h := \text{col}(h_x, h_y, h_u) \in \mathbb{R}^{n_{\text{ineq}}}, \quad (9f)$$

with  $n_{\text{eq}} = p + n + r_x + r_y + r_u$ ,  $n_{\text{ineq}} = k_x + k_y + k_u$ ,  $R_{\text{eq},x} := \text{blkdiag}(R_{\text{eq},x,1}, \dots, R_{\text{eq},x,N})$ ,  $b_x := \text{col}(b_{x,1}, \dots, b_{x,N})$ ,  $R_{\text{ineq},x} := \text{blkdiag}(R_{\text{ineq},x,1}, \dots, R_{\text{ineq},x,N})$ , and  $h_x := \text{col}(h_{x,1}, \dots, h_{x,N})$ . The remaining block matrices and vectors, namely  $R_{\text{eq},y}$ ,  $R_{\text{eq},u}$ ,  $R_{\text{ineq},y}$ ,  $R_{\text{ineq},u}$ ,  $b_y$ ,  $b_u$ ,  $h_y$  and  $h_u$  are defined analogously.

The following technical assumptions about the optimization problem (9) are instrumental for showing the existence of a unique solution to (9), as well as for establishing strict shifted-passivity properties for the corresponding Aug-PDGD with respect to a suitable input-output pair.

*Assumption 4:* The cost function  $J$  in (8) is twice continuously differentiable,  $\mu$ -strongly convex, and  $\ell$ -smooth in its arguments, for some  $0 < \mu \leq \ell$ .  $\square$

Assumption 4 implies that, in particular, for all  $\xi_1, \xi_2 \in \mathbb{R}^{n+m+p}$ , it holds that

$$\mu \|\xi_1 - \xi_2\|^2 \leq \langle \nabla J(\xi_1) - \nabla J(\xi_2), \xi_1 - \xi_2 \rangle \leq \ell \|\xi_1 - \xi_2\|^2,$$

or, equivalently,  $\mu \mathbf{I} \preceq \nabla^2 J(\xi) \preceq \ell \mathbf{I}$  for all  $\xi \in \mathbb{R}^{n+m+p}$ .

*Assumption 5:* Let  $n_c := n_{\text{eq}} + n_{\text{ineq}}$ . The stacked constraint matrix

$$R = \begin{bmatrix} R_{\text{eq}} \\ R_{\text{ineq}} \end{bmatrix} \quad (10)$$

has full row rank.  $\square$

With Assumption 5, there exist constants  $0 < \kappa_1 \leq \kappa_2$  such that

$$\kappa_1 \mathbf{I} \leq RR^\top \leq \kappa_2 \mathbf{I}, \quad (11)$$

where  $RR^\top \in \mathbb{R}^{n_c \times n_c}$ .

In view of Assumption 4 and the fact that the constraints are affine in the decision variables, the optimization problem (9) is convex. Then, it is solvable if and only if the following KKT conditions [18] are solvable:

$$\begin{aligned} \nabla J(\bar{\xi}) + R_{\text{eq}}^\top \bar{\nu}_{\text{eq}} + R_{\text{ineq}}^\top \bar{\nu}_{\text{ineq}} &= \mathbf{0}, \\ R_{\text{eq}} \bar{\xi} - b &= \mathbf{0}, \\ R_{\text{ineq}} \bar{\xi} - h &\leq \mathbf{0}, \\ \bar{\nu}_{\text{ineq}} &\geq \mathbf{0}, \\ \bar{\nu}_{\text{ineq}}^\top (R_{\text{ineq}} \bar{\xi} - h) &= \mathbf{0}, \end{aligned} \quad (12)$$

where  $\bar{\nu}_{\text{eq}} \in \mathbb{R}^{n_{\text{eq}}}$  and  $\bar{\nu}_{\text{ineq}} \in \mathbb{R}_{\geq 0}^{n_{\text{ineq}}}$  are dual variables. Under Assumptions 4 and 5, the KKT conditions (12) admit a unique solution [18]. In order to define the Aug-PDGD associated to (9) and (12), we follow [11] and introduce the augmented Lagrangian function

$$\begin{aligned} \mathcal{L}_\rho(\bar{\xi}, \bar{\nu}_{\text{eq}}, \bar{\nu}_{\text{ineq}}) &= J(\bar{\xi}) + \bar{\nu}_{\text{eq}}^\top (R_{\text{eq}} \bar{\xi} - b) \\ &+ \sum_{i=1}^{n_{\text{ineq}}} H_\rho((R_{\text{ineq}} \bar{\xi} - h)_i, (\bar{\nu}_{\text{ineq}})_i), \end{aligned} \quad (13)$$

where  $H_\rho$  is defined as

$$H_\rho(a, b) = \begin{cases} ab + \frac{\rho}{2}a^2 & \rho a + b \geq 0, \\ -\frac{b^2}{2\rho}, & \rho a + b < 0, \end{cases} \quad (14)$$

with  $\rho > 0$  being a free parameter. Then, the Aug-PDGD is defined as follows [11]:

$$\dot{\xi} = -\nabla_{\xi} \mathcal{L}(\xi, \nu_{\text{eq}}, \nu_{\text{ineq}}), \quad (15a)$$

$$\dot{\nu}_{\text{eq}} = \eta \nabla_{\nu_{\text{eq}}} \mathcal{L}(\xi, \nu_{\text{eq}}, \nu_{\text{ineq}}), \quad (15b)$$

$$\dot{\nu}_{\text{ineq}} = \eta \nabla_{\nu_{\text{ineq}}} \mathcal{L}(\xi, \nu_{\text{eq}}, \nu_{\text{ineq}}), \quad (15c)$$

where  $\xi(t) = \text{col}(\hat{x}(t), \hat{y}(t), \hat{u}(t))$ ,  $\nu_{\text{eq}}(t)$  and  $\nu_{\text{ineq}}(t)$  are the virtual states associated to the primal ( $\bar{\xi} = \text{col}(\bar{x}, \bar{y}, \bar{u})$ ) and dual variables ( $\bar{\nu}_{\text{eq}}$ ,  $\bar{\nu}_{\text{ineq}}$ ), and  $\eta > 0$  is a design parameter. Note that under Assumptions 4 and 5, the Aug-PDGD (15) admits a unique equilibrium, which is in one-to-one correspondence with the unique solution of the KKT conditions (12).

We underscore that in [11], a PDGD with affine equality constraints and an Aug-PDGD with affine inequality constraints are analyzed separately, and it is noted that they can be combined. Building on their results, here we consider an Aug-PDGD that deals with affine equality and inequality constraints simultaneously.

To write (15) in explicit form, note that

$$\begin{aligned} \nabla_{\xi} \mathcal{L}(\xi, \nu_{\text{eq}}, \nu_{\text{ineq}}) &= \nabla_{\xi} J(\xi) + R_{\text{eq}}^{\top} \nu_{\text{eq}} \\ &\quad + \sum_{i=1}^{n_{\text{ineq}}} \nabla_{\xi} H_{\rho}((R_{\text{ineq}} \xi - h)_i, (\nu_{\text{ineq}})_i), \\ \nabla_{\nu_{\text{eq}}} \mathcal{L}(\xi, \nu_{\text{eq}}, \nu_{\text{ineq}}) &= R_{\text{eq}} \xi - b, \\ \nabla_{\nu_{\text{ineq}}} \mathcal{L}(\xi, \nu_{\text{eq}}, \nu_{\text{ineq}}) &= \sum_{i=1}^{n_{\text{ineq}}} \nabla_{\nu_{\text{ineq}}} H_{\rho}((R_{\text{ineq}} \xi - h)_i, (\nu_{\text{ineq}})_i). \end{aligned}$$

To compute the remaining terms with derivatives of  $H_{\rho}$ , we introduce, as in [11], the vector

$$g(\xi, \nu_{\text{ineq}}) := \max\left(\nu_{\text{ineq}} + \rho(R_{\text{ineq}} \xi - h), 0\right), \quad (17)$$

where the  $\max(\cdot)$  is taken component-wise. Then,

$$\begin{aligned} \sum_{i=1}^{n_{\text{ineq}}} \nabla_{\xi} H_{\rho}((R_{\text{ineq}} \xi - h)_i, (\nu_{\text{ineq}})_i) &= R_{\text{ineq}}^{\top} g(\xi, \nu_{\text{ineq}}), \\ \sum_{i=1}^{n_{\text{ineq}}} \nabla_{\nu_{\text{ineq}}} H_{\rho}((R_{\text{ineq}} \xi - h)_i, (\nu_{\text{ineq}})_i) &= \frac{1}{\rho} (g(\xi, \nu_{\text{ineq}}) - \nu_{\text{ineq}}). \end{aligned}$$

Consequently, the Aug-PDGD attains the following form:

$$\dot{\theta} = f(\theta), \quad \theta = \text{col}(\xi, \nu_{\text{eq}}, \nu_{\text{ineq}}) \in \mathbb{R}^{n_{\theta} = n_{\xi} + n_{\text{eq}} + n_{\text{ineq}}}, \quad (18a)$$

with

$$f(\theta) = \begin{pmatrix} -\nabla J(\xi) - R_{\text{eq}}^{\top} \nu_{\text{eq}} - R_{\text{ineq}}^{\top} g(\xi, \nu_{\text{ineq}}) \\ \eta(R_{\text{eq}} \xi - b) \\ \frac{\eta}{\rho} (g(\xi, \nu_{\text{ineq}}) - \nu_{\text{ineq}}) \end{pmatrix}. \quad (18b)$$

### B. Aug-PDGD-based CbI Framework

To apply the CbI framework, we first equip the Aug-PDGD (18) with an auxiliary input  $v_{\text{pd}}$  as follows:

$$\Sigma_c : \quad \dot{\theta} = f(\theta) + B_{\text{pd}} v_{\text{pd}}, \quad (19)$$

where  $B_{\text{pd}}$  is the associated input matrix (to be defined). Next, we move on to show that (19) is strictly shifted-passive with quadratic storage function, and with respect to a suitable output. In the sequel, the passive input-output pairs of both the CPS model (3) and the Aug-PDGD (19) will be used to define a power-preserving interconnection between the two systems.

To establish the shifted-passivity property for  $\Sigma_c$ , we consider the quadratic storage function (candidate)  $S_c = \tilde{\theta}^{\top} P_2 \tilde{\theta}$ , where  $P_2$  is a symmetric matrix defined as

$$P_2 = \begin{bmatrix} \eta c \mathbf{I} & \eta R_{\text{eq}}^{\top} & \eta R_{\text{ineq}}^{\top} \\ \eta R_{\text{eq}} & c \mathbf{I} & \mathbf{0} \\ \eta R_{\text{ineq}} & \mathbf{0} & c \mathbf{I} \end{bmatrix} \in \mathbb{R}^{n_{\theta} \times n_{\theta}}, \quad (20)$$

with  $R_{\text{eq}}$  and  $R_{\text{ineq}}$  as in (9c) and

$$c = \max(c_1, c_2, c_3), \quad (21a)$$

$$c_1 \geq \begin{cases} \eta \sqrt{\frac{\kappa_2}{(\eta - \epsilon)(1 - \epsilon)}}, & \eta \geq 1, \\ \sqrt{\frac{\eta \kappa_2}{(1 - \epsilon)(1 - \eta\epsilon)}}, & 0 < \eta < 1, \end{cases} \quad (21b)$$

$$c_2 \geq \kappa_2 \rho, \quad (21c)$$

$$c_3 \geq 20 \ell \left[ \max\left(\frac{\rho \kappa_2}{\mu}, \frac{\ell}{\mu}\right) \right]^2 \left[ \max\left(\frac{\eta}{\ell \rho}, \frac{\ell}{\mu}\right) \right]^2 \frac{\kappa_2}{\kappa_1}, \quad (21d)$$

with  $0 < \epsilon < 1$  being a free parameter, and where  $\ell$  and  $\mu$  are the smoothness and strong-convexity constants of  $J$  from Assumption 4,  $\kappa_1, \kappa_2$  are the spectral bounds of  $RR^\top$  from Assumption 5, and  $\rho > 0$  is the free parameter introduced in (14).

*Lemma 2:* Fix  $\eta > 0$  and  $\epsilon \in (0, 1)$ , let Assumptions 4 and 5 hold, and fix  $c > 0$  according to (21). Then,  $P_2$  in (20) satisfies

$$P_2 \succeq \epsilon c \min(\eta, 1) \mathbf{I}. \quad (22)$$

Moreover, the Aug-PDGD (19) is strictly shifted-passive with quadratic storage function  $S_c(\tilde{\theta}) = \tilde{\theta}^\top P_2 \tilde{\theta}$  and with respect to the input–output pair  $(\tilde{v}_{\text{pd}}, 2 B_{\text{pd}}^\top P_2 \tilde{\theta})$ . In particular, it holds that

$$\dot{S}_c \leq -\tau_2 \tilde{\theta}^\top P_2 \tilde{\theta} + 2 \tilde{\theta}^\top P_2 B_{\text{pd}} \tilde{v}_{\text{pd}}$$

along any system trajectory, with

$$\tau_2 := \frac{\eta \kappa_1}{2c}. \quad (23)$$

□

**Proof.** See Appendix A. ■

In view of Lemmas 1 and 2, we are in position to specify the interconnection law between the CPS (3) and the Aug-PDGD with input (19) as follows:

$$\Sigma_{\text{I}} : \begin{cases} u = M_u \theta, \\ v_{\text{pd}} = -(y - M_y \theta), \end{cases} \quad (24a)$$

$$(24b)$$

where

$$M_u = 2B_{\text{pd}}^\top P_2 = [\mathbf{0}_{m \times n+p} \quad \mathbf{I}_{m \times m} \quad \mathbf{0}_{m \times n_{\text{eq}} + n_{\text{ineq}}}], \quad (25a)$$

$$M_y = [\mathbf{0}_{p \times n} \quad \mathbf{I}_{p \times p} \quad \mathbf{0}_{p \times m + n_{\text{eq}} + n_{\text{ineq}}}], \quad (25b)$$

with  $B_{\text{pd}}$  and  $P_2$  defined in (19) and (20), respectively. With the proposed choice of  $M_u$ , it is straightforward to verify that  $M_u \theta = \hat{u}$ . Then, (24) implies that the input to the CPS (3) is assigned to be equal to the passive output of the Aug-PDGD. Moreover,  $M_y$  is such that  $M_y \theta = \hat{y}$ , where  $\hat{y}$  is the Aug-PDGD estimate of the passive output  $y$  of the CPS dynamics (3). Then, (24) implies that  $v_{\text{pd}}$  vanishes at equilibrium, making the closed-loop system's equilibrium coincide with the solution of the KKT conditions (12). In essence, (24) is a feedback, power-preserving interconnection between two (strictly) shifted-passive systems. Finally, note that  $B_{\text{pd}}$  can be computed as  $B_{\text{pd}} = \frac{1}{2} P_2^{-1} M_u^\top$ .

## V. CONDITIONS FOR CLOSED-LOOP STABILITY

In this section, we provide sufficient tuning conditions for the controller (19), (24) under which the overall closed-loop system, conformed by (3), (19) and (24), possesses a unique globally exponentially stable equilibrium.

*Theorem 1:* Consider the closed-loop system  $\Sigma_{\text{cl}} = \Sigma_{\text{p}} \circ \Sigma_{\text{I}} \circ \Sigma_{\text{c}}$ . Let

$$\beta := \max_i \{(\lambda_i(M_u^\top M_y + M_y^\top M_u))\}. \quad (26)$$

Choose  $\eta > 0$  such that, with  $\epsilon$  as defined in (21b),

$$\eta \kappa_1 \epsilon \min(\eta, 1) > \beta. \quad (27)$$

Then, the unique equilibrium point of the closed-loop system  $\Sigma_{\text{cl}}$  is exponentially stable with decay rate no slower than

$$\tau = \frac{1}{2} \min(\tau_1, \tau_{2,e}), \quad (28a)$$

where  $0 < \tau_1 < 2 \min_i \{-\text{Re}(\lambda_i(A_p))\}$  and, with  $c$  from (21),

$$\tau_{2,e} = \frac{2\tau_2 \epsilon c \min(\eta, 1) - \beta}{2\epsilon c \min(\eta, 1)}. \quad (28b)$$

□

**Proof.** Consider the Lyapunov function  $S := S_p + S_c$ , where  $S_p$  and  $S_c$  are as in Lemmas 1 and 2, respectively. Along any trajectory of  $\Sigma_{\text{cl}}$ ,  $\dot{S}$  satisfies, in view of Lemmas 1 and 2,

$$\dot{S} \leq -\tau_1 \tilde{x}^\top P_1 \tilde{x} + \tilde{y}^\top \tilde{u} - \tau_2 \tilde{\theta}^\top P_2 \tilde{\theta} + 2 \tilde{\theta}^\top P_2 B_{\text{pd}} \tilde{v}_{\text{pd}}. \quad (29)$$

Due to the interconnection (24), the inequality (29) simplifies to

$$\dot{S} \leq -\tau_1 \tilde{x}^\top P_1 \tilde{x} - \tau_2 \tilde{\theta}^\top P_2 \tilde{\theta} + \tilde{\theta}^\top M_u^\top M_y \tilde{\theta}. \quad (30)$$

Let

$$\beta = \max_i \{(\lambda_i(M_u^\top M_y + M_y^\top M_u))\}.$$

Then,

$$\tilde{\theta}^\top M_u^\top M_y \tilde{\theta} \leq \frac{\beta}{2} \|\tilde{\theta}\|^2. \quad (31)$$

Due to (67), it holds that

$$\|\tilde{\theta}\|^2 \leq \frac{1}{\epsilon c \min(\eta, 1)} \tilde{\theta}^\top P_2 \tilde{\theta}. \quad (32)$$

By combining (32) with (31) we obtain that

$$\tilde{\theta}^\top M_u^\top M_y \tilde{\theta} \leq \frac{\beta}{2 \epsilon c \min(\eta, 1)} \tilde{\theta}^\top P_2 \tilde{\theta}. \quad (33)$$

Considering (33), the following inequality is implied from (30):

$$\dot{S} \leq -\tau_1 \tilde{x}^\top P_1 \tilde{x} - \left(\tau_2 - \frac{\beta}{2 \epsilon c \min(\eta, 1)}\right) \tilde{\theta}^\top P_2 \tilde{\theta}. \quad (34)$$

From Lemma 2,  $\tau_2 = \frac{\eta \kappa_1}{2c}$ . Then,

$$\tau_2 - \frac{\beta}{2 \epsilon c \min(\eta, 1)} = \frac{\eta \kappa_1}{2c} - \frac{\beta}{2 \epsilon c \min(\eta, 1)}.$$

Note that if  $\eta \geq 1$ , then  $\min(\eta, 1) = 1$ , and

$$\frac{\eta \kappa_1}{2c} - \frac{\beta}{2 \epsilon c} = \frac{\eta \kappa_1 \epsilon - \beta}{2 \epsilon c}.$$

The right-hand side of this equation is positive due to (27). Alternatively, if  $0 < \eta < 1$ , then  $\min(\eta, 1) = \eta$ , and

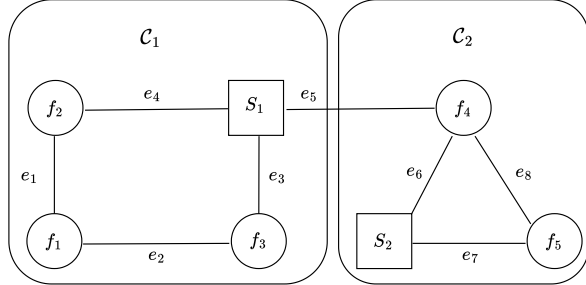
$$\frac{\eta \kappa_1}{2c} - \frac{\beta}{2 \epsilon c \eta} = \frac{\eta^2 \kappa_1 \epsilon - \beta}{2 \epsilon c}.$$

Analogously, the right-hand side of this equation is positive due to (27). It follows that under the condition of the theorem  $\tau_2 - \frac{\beta}{2 \epsilon c \min(\eta, 1)} > 0$ . Then, choosing  $\tau_{2,e} > 0$  as in (28b) ensures that

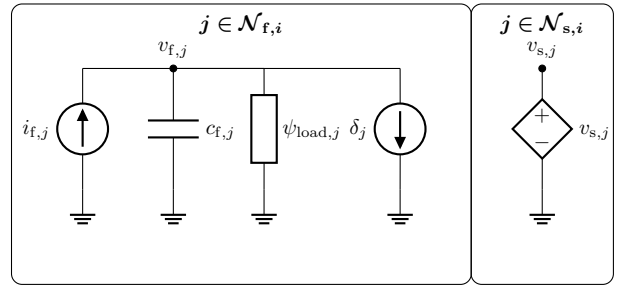
$$\dot{S} \leq -\tau_1 \tilde{x}^\top P_1 \tilde{x} - \tau_{2,e} \tilde{\theta}^\top P_2 \tilde{\theta}.$$

Consequently, the unique equilibrium of the closed-loop system  $\Sigma_{\text{cl}}$  is exponentially stable. Moreover, the decay rate is no slower than  $\tau = \frac{1}{2} \min(\tau_1, \tau_{2,e})$  [13, Theorem 4.10]. ■

*Remark 1:* Assume that at each fault-induced switching instant the Lyapunov function  $S$  may increase by at most a factor  $\gamma_f \geq 1$ , i.e.,  $S(t_k^+) \leq \gamma_f S(t_k^-)$ . Between switches, each mode (i.e., the closed-loop dynamics obtained by interconnecting (3), (19), and (24) for a fixed fault configuration) has an exponentially stable equilibrium with decay rate  $\tau > 0$ , i.e.,  $\dot{S} \leq -2\tau S$ . Then, a sufficient dwell-time ensuring overall exponential stability, even under consecutive faults, is given by  $T_{\text{dwell}} > \frac{\ln \gamma_f}{2\tau}$ , which follows from standard average dwell-time arguments for switched systems with multiple Lyapunov functions [19, Theorem 3.2]. □



(a) DC microgrid partitioned into two clusters  $\mathcal{C}_1$  and  $\mathcal{C}_2$ .



(b) Schematic of voltage-following (left) and voltage-setting (right) buses.

Fig. 1: System overview: (a) DC microgrid partitioned into clusters and (b) bus-type schematic.

## VI. APPLICATION TO DC MICROGRIDS

Driven by environmental goals, the growing penetration of renewables is accelerating the adoption of flexible distribution architectures such as microgrids. Microgrids comprise interconnected distributed generation unit (DGU)s, storage units, and loads, and can operate grid-connected or islanded [20]; here we focus on the islanded case. Microgrids remain vulnerable to faults that can degrade performance or compromise stability, motivating robust and FTC strategies [21]. The FTC framework developed in this paper for general CPSs is well suited to address these challenges, as illustrated next on a representative DC microgrid example.

### A. System Model

Consider a network of  $n \geq 1$  DC microgrid clusters  $\mathcal{C}_1, \dots, \mathcal{C}_n$  interconnected via tie-lines; see Fig. 1a for an illustrative example with two clusters. We model each cluster  $\mathcal{C}_i$  as an arbitrarily oriented graph  $\mathcal{G}_i = (\mathcal{N}_i, \mathcal{E}_i)$ , where each element in  $\mathcal{N}_i$  represents an electric bus, and each element in  $\mathcal{E}_i$ , an inductive-resistive power line. We consider the following splitting of the elements in  $\mathcal{N}_i$  and  $\mathcal{E}_i$ :

$$\begin{aligned}\mathcal{N}_i &= \mathcal{N}_{s,i}^a \cup \mathcal{N}_{f,i}^a \cup \mathcal{N}_{s,i}^b \cup \mathcal{N}_{f,i}^b \\ \mathcal{E}_i &= \mathcal{E}_i^a \cup \mathcal{E}_i^{ab}.\end{aligned}$$

Each element  $j \in \mathcal{N}_{s,i}^a$  represents an electric bus *within* the cluster  $\mathcal{C}_i$ , whose voltage  $v_{s,j}$  is directly assigned by a voltage-setting DGU. We assume that each cluster has at least one voltage-setting bus, i.e.,  $|\mathcal{N}_{s,i}^a| \geq 1$ . Each element  $j \in \mathcal{N}_{f,i}^a$  represents a capacitive bus, also within the cluster  $\mathcal{C}_i$ , with voltage  $v_{f,j}$  and capacitance  $c_{f,j}$ , to which a voltage-following DGU directly injects a current  $i_{f,j}$ , and which energizes a ZI-load with admittance  $\psi_{load,j}$  and constant-current term  $\delta_{load,j}$ . Analogous descriptions follow for the elements in  $\mathcal{N}_{s,i}^b$  and  $\mathcal{N}_{f,i}^b$ , with the distinction that their elements are associated to buses of any other cluster different from  $\mathcal{C}_i$  which is physically linked to  $\mathcal{C}_i$  via a tie-line.

Each tie-line is assigned to exactly one of its incident clusters. Tie-lines never connect two voltage-setting buses; if a tie-line connects a voltage-setting bus to a voltage-following bus, it is assigned to the cluster containing the voltage-setting bus. Accordingly,  $\mathcal{E}_i^a$  collects all lines owned by  $\mathcal{C}_i$  (internal lines and assigned tie-lines), whereas  $\mathcal{E}_i^{ab}$  contains tie-lines incident to  $\mathcal{C}_i$  but assigned to adjacent clusters. Accordingly,  $\mathcal{E}_i^a \subset (\mathcal{N}_i^a \times \mathcal{N}_i^a) \cup (\mathcal{N}_i^a \times \mathcal{N}_i^b)$ . Alternatively, each element in  $\mathcal{E}_i^{ab}$  represents a tie-line linking a bus within cluster  $\mathcal{C}_i$  to a bus  $k \in \mathcal{N}_i^b$  belonging to an adjacent cluster, *and assigned to that adjacent cluster*, i.e.,  $\mathcal{E}_i^{ab} \subset \mathcal{N}_i^a \times \mathcal{N}_i^b$ . The current and inductance–resistance pair of such lines adopts the same notation as for the elements in  $\mathcal{E}_i^a$ .

For each cluster  $\mathcal{C}_i$ , let us introduce the vectors  $V_{s,a,i} = \text{col}(\{v_{s,j}\}_{j \in \mathcal{N}_{s,i}^a})$  and  $V_{f,a,i} = \text{col}(\{v_{f,j}\}_{j \in \mathcal{N}_{f,i}^a})$ , with analogous definitions holding for  $V_{s,b,i}$  and  $V_{f,b,i}$ . Moreover, let  $I_{a,i} = \text{col}(\{i_{line,j}\}_{j \in \mathcal{E}_i^a})$  and  $I_{ab,i} = \text{col}(\{i_{line,j}\}_{j \in \mathcal{E}_i^{ab}})$ . By introducing the node-edge incidence matrix  $\mathcal{B}_i$  for cluster  $\mathcal{C}_i$  as

$$\mathcal{B}_i^\top = \begin{bmatrix} (\mathcal{B}_{s,a,i}^a)^\top & (\mathcal{B}_{f,a,i}^a)^\top & (\mathcal{B}_{s,b,i}^a)^\top & (\mathcal{B}_{f,b,i}^a)^\top \\ (\mathcal{B}_{s,a,i}^{ab})^\top & (\mathcal{B}_{f,a,i}^{ab})^\top & (\mathcal{B}_{s,b,i}^{ab})^\top & (\mathcal{B}_{f,b,i}^{ab})^\top \end{bmatrix},$$

then it is possible to obtain the following dynamical model for  $\mathcal{C}_i$ :

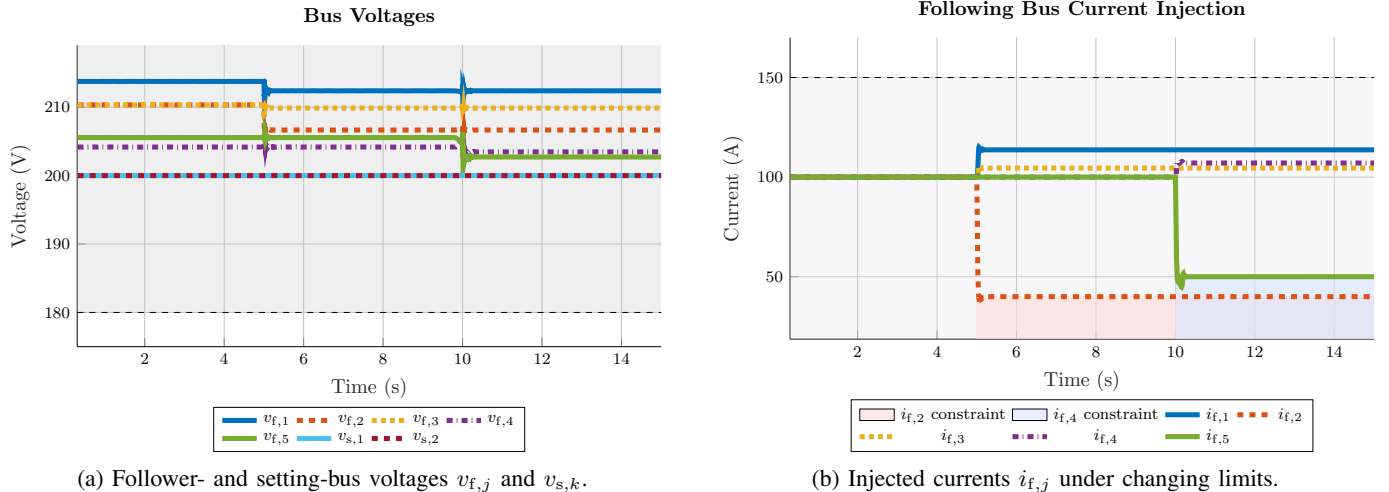


Fig. 2: Closed-loop trajectories of the DC microgrid under the proposed FTC scheme.

$$C_{f,a,i} \dot{V}_{f,a,i} = -Y_{load,i} V_{f,a,i} - I_{load,i} + I_{f,a,i} - \mathcal{B}_{f,a,i}^a I_{a,i} - \mathcal{B}_{f,a,i}^{ab} I_{ab,i}, \quad (35a)$$

$$L_{a,i} \dot{I}_{a,i} = -R_{a,i} I_{a,i} + (\mathcal{B}_{s,a,i}^a)^\top V_{s,a,i} + (\mathcal{B}_{f,a,i}^a)^\top V_{f,a,i} + (\mathcal{B}_{f,b,i}^a)^\top V_{f,b,i}, \quad (35b)$$

where  $C_{f,a,i} = \text{diag}(\{c_{f,j}\}_{j \in \mathcal{N}_{f,i}^a})$ ,  $Y_{load,i} = \text{diag}(\{\psi_{load,j}\}_{j \in \mathcal{N}_{f,i}^a})$ ,  $I_{load,i} = \text{col}(\{\delta_{load,j}\}_{j \in \mathcal{N}_{f,i}^a})$  and  $I_{f,a,i} = \text{col}(\{i_{f,j}\}_{j \in \mathcal{N}_{f,i}^a})$ ; moreover,  $L_{a,i} = \text{diag}(\{\ell_{line,j}\}_{j \in \mathcal{E}_i^a})$  and  $R_{a,i} = \text{diag}(\{r_{line,j}\}_{j \in \mathcal{E}_i^a})$ . The model (35) can be written in the state space form (1) by defining the state vector  $x_i = \text{col}(V_{f,a,i}, I_{a,i})$ , the measured output  $y_i = \text{col}(V_{f,a,i}, I_{a,i})$ , the interconnection output  $z_i = \text{col}(\mathcal{B}_{f,a,i}^a V_{f,a,i}, \mathcal{B}_{f,b,i}^a I_{a,i})$ , the vector of control inputs  $u_i = \text{col}(I_{f,a,i}, V_{s,a,i})$ , the vector of external variables  $w_i = \text{col}(I_{ab,i}, V_{f,b,i})$ , with  $(A_i, B_i, d_i, G_i, E_i, C_i)$  defined accordingly. Moreover, the admissible steady-state sets for each cluster  $\mathcal{C}_i$  are  $\mathcal{X}_i := \{x_i \mid V_{f,a,i} \geq V_{f,a,i}^{\min}\}$ ,  $\mathcal{U}_i := \{u_i \mid I_{f,a,i} \leq I_{f,a,i}^{\max}, V_{s,a,i} \geq V_{s,a,i}^{\min}\}$ , and  $\mathcal{Y}_i := \{y_i \mid y_i = x_i, V_{f,a,i} \geq V_{f,a,i}^{\min}\}$ .

The interconnection between clusters  $\mathcal{C}_i$  and  $\mathcal{C}_j$  is

$$\Omega_{ij} := \begin{bmatrix} \mathbf{0} & -P_{ij}^i \\ P_{ij}^v & \mathbf{0} \end{bmatrix},$$

where  $P_{ij}^v$  and  $P_{ij}^i$  are Boolean selection matrices encoding the tie-line adjacency.<sup>8</sup> By consistent stacking of shared tie-lines, the selection matrices satisfy  $P_{ij}^i = (P_{ji}^v)^\top$  (equivalently  $P_{ij}^v = (P_{ji}^i)^\top$ ), hence  $\Omega_{ij} + \Omega_{ji}^\top = \mathbf{0}$  and Assumption 2 holds.

### B. Fault Scenario and Numerical Simulations

We focus on faults that manifest as a power loss at a voltage-following bus. Then, for some voltage-following DGU  $j \in \mathcal{N}_{f,i}^a$  within a cluster  $\mathcal{C}_i$ , a step reduction in the current injection  $i_{f,j}$  occurs at time  $t_f$ . Consequently, the objective of the FTC (19), (24), applied to the DC microgrid model, is to drive the system towards a new equilibrium whose error with respect to the pre-fault pre-fault equilibrium is minimum, while respecting all physical and fault-induced constraints. The desired post-fault steady-state is a solution to an optimization problem of the form (9), with cost function

$$J(\bar{\xi}) = \|\bar{\xi} - \xi^*\|_K^2,$$

with  $\xi^* = \text{col}(x^*, u^*)$ ,  $\bar{\xi} = \text{col}(\bar{x}, \bar{u})$ ,  $K = \text{blkdiag}(K_x, K_u) \succ \mathbf{0}$ , and steady-state equality and inequality constraints given by  $R_{\text{eq}} \bar{\xi} = b$  and  $R_{\text{ineq}} \bar{\xi} \leq h$ , with

$$R_{\text{eq}} = \begin{bmatrix} -Y_{load} & -\mathcal{B}_f & \mathbf{I} & \mathbf{0} \\ (\mathcal{B}_f)^\top & -R_a & \mathbf{0} & (\mathcal{B}_s)^\top \end{bmatrix}, \quad b = \begin{bmatrix} I_{load} \\ \mathbf{0} \end{bmatrix},$$

<sup>7</sup>From a practical standpoint, we impose lower bounds on the setting-bus voltages to avoid undervoltage and upper bounds on the follower-bus injected currents to respect source current ratings, which may become tighter after a fault.

<sup>8</sup> $P_{ij}^v$  selects the boundary-bus voltages of  $\mathcal{C}_j$  that appear as remote voltages in  $V_{f,b,i}$ , and  $P_{ij}^i$  selects the tie-line currents owned by  $\mathcal{C}_j$  that appear as incident (non-owned) currents in  $I_{ab,i}$ . The minus sign enforces opposite current-flow conventions at the two ends of each tie-line.

$$R_{\text{ineq}} = \begin{bmatrix} \mathbf{0} & \mathbf{0} & \mathbf{I} & \mathbf{0} \\ \mathbf{0} & \mathbf{0} & \mathbf{0} & -\mathbf{I} \end{bmatrix}, \quad h = \begin{bmatrix} I_f^{\max} \\ -V_s^{\min} \end{bmatrix},$$

where  $Y_{\text{load}} := \text{blkdiag}(Y_{\text{load},1}, \dots, Y_{\text{load},n})$ ,  $R_a := \text{blkdiag}(R_{a,1}, \dots, R_{a,n})$ ,  $I_{\text{load}} := \text{col}(I_{\text{load},1}, \dots, I_{\text{load},n})$ . Moreover,  $\mathcal{B}_f$  and  $\mathcal{B}_s$  denote the global node–edge incidence matrices corresponding to the voltage-following and voltage-setting buses, respectively.

For the numerical experiments, we consider the DC microgrid shown in Fig. 1a. All parameters defining the system model and the steady-state operational constraints are provided in the accompanying online repository [22]<sup>9</sup>. Figure 2 shows the trajectories of  $i_f$ , and the bus voltages  $v_f, v_s$ . At  $t = 5\text{s}$ , the voltage-following bus 2 loses power capacity, reducing its injection limit from 150 A to 40 A; at  $t = 10\text{s}$ , the voltage-following bus 5 is reduced to 50 A. Despite these faults, the proposed FTC keeps voltages and currents within bounds and converges to a feasible operating point close to the pre-fault one.

## VII. CONCLUSIONS

In this paper, we have presented an active primal-dual FTC scheme based on an Aug-PDGD for the post-fault exponential stabilization of a class of networked CPS. The proposed approach—which is framed as a CbI control scheme—was designed to provably achieve convergence towards the unique (KKT) solution of a constrained optimization problem encoding desired post-fault operation. This addresses the lack, highlighted in the literature review, of network-level, constraint-aware optimal coordination with explicit optimality guarantees under shared-resource and interconnection constraints in CPS such as power and energy networks (e.g., microgrids). Numerical simulations on a representative DC microgrid showed that the proposed method ensures post-fault closed-loop stability and maintains pre-specified steady-state operational constraints (such as bus-voltage and line-current limits) in the presence of non-trivial faults, such as loss of power capacity at the generation units. Future work will focus on providing conditions for enabling a distributed implementation of the proposed controller and on its real-time experimental validation in a power hardware-in-the-loop environment.

## ACKNOWLEDGMENT

This work builds on earlier unpublished work conducted while the second author was at University of Groningen (2020-2023). We acknowledge S. Ahmed, J. Ferguson, M. Cucuzzella and J.M.A. Scherpen for their contributions to those efforts.

## REFERENCES

- [1] R. M. G. Ferrari and A. M. H. Teixeira, *Safety, security and privacy for cyber-physical systems*. Springer, 2021.
- [2] X.-M. Zhang, Q.-L. Han, X. Ge, D. Ding, L. Ding, D. Yue, and C. Peng, “Networked control systems: A survey of trends and techniques,” *IEEE/CAA Journal of Automatica Sinica*, vol. 7, no. 1, pp. 1–17, 2020.
- [3] Y. Zhang and J. Jiang, “Bibliographical review on reconfigurable fault-tolerant control systems,” *Annual Reviews in Control*, vol. 32, no. 2, pp. 229–252, 2008.
- [4] F. Boem, A. J. Gallo, D. M. Raimondo, and T. Parisini, “Distributed fault-tolerant control of large-scale systems: An active fault diagnosis approach,” *IEEE Transactions on Control of Network Systems*, vol. 7, no. 1, pp. 288–301, 2020.
- [5] A. Van der Schaft, *L2-gain and passivity techniques in nonlinear control*. Springer, 2000.
- [6] R. Ortega and E. Garcia-Canseco, “Interconnection and damping assignment passivity-based control: A survey,” *European Journal of control*, vol. 10, no. 5, pp. 432–450, 2004.
- [7] K. Schenk, B. Gülbitti, and J. Lunze, “Cooperative fault-tolerant control of networked control systems,” *IFAC-PapersOnLine*, vol. 51, no. 24, pp. 570–577, 2018, 10th IFAC Symposium on Fault Detection, Supervision and Safety for Technical Processes (SAFEPROCESS 2018).
- [8] K. Schenk and J. Lunze, “Fault tolerance in networked systems through flexible task assignment,” in *2019 4th Conference on Control and Fault Tolerant Systems (SysTol)*, 2019, pp. 257–263.
- [9] ———, “Fault-tolerant task allocation in networked control systems,” in *2020 28th Mediterranean Conference on Control and Automation (MED)*, 2020, pp. 313–318.
- [10] C.-H. Xie and G.-H. Yang, “Decentralized adaptive fault-tolerant control for large-scale systems with external disturbances and actuator faults,” *Automatica*, vol. 85, pp. 83–90, 2017.
- [11] G. Qu and N. Li, “On the exponential stability of primal-dual gradient dynamics,” *IEEE Control Systems Letters*, vol. 3, no. 1, pp. 43–48, 2019.
- [12] R. Ortega, A. van der Schaft, F. Castanos, and A. Astolfi, “Control by interconnection and standard passivity-based control of port-Hamiltonian systems,” *IEEE Transactions on Automatic Control*, vol. 53, no. 11, pp. 2527–2542, 2008.
- [13] H. Khalil, *Nonlinear Systems*. Prentice Hall, 2002, vol. 3.
- [14] T. W. Stegink, C. De Persis, and A. J. van der Schaft, “Stabilization of structure-preserving power networks with market dynamics,” *IFAC-PapersOnLine*, vol. 50, no. 1, pp. 6737–6742, 2017, 20th IFAC World Congress.
- [15] K. C. Kosaraju, M. Cucuzzella, and J. M. A. Scherpen, “Distributed control of DC microgrids using primal-dual dynamics,” in *2019 IEEE 58th Conference on Decision and Control (CDC)*, 2019, pp. 6215–6220.
- [16] M. Colombino, E. Dall’Anese, and A. Bernstein, “Online optimization as a feedback controller: Stability and tracking,” *IEEE Transactions on Control of Network Systems*, vol. 7, no. 1, pp. 422–432, 2020.
- [17] A. Hauswirth, Z. He, S. Bolognani, G. Hug, and F. Dörfler, “Optimization algorithms as robust feedback controllers,” *Annual Reviews in Control*, vol. 57, p. 100941, 2024.
- [18] S. Boyd and L. Vandenberghe, *Convex optimization*. Cambridge University Press, 2004.
- [19] D. Liberzon, *Switching in systems and control*. Springer, 2003, vol. 190.

<sup>9</sup>Using these values, it can be verified that the assumptions and design conditions stated in this paper are satisfied for the considered system.

- [20] Cucuzzella, Michele, Scherpen, Jacquelien M. A., and Machado, Juan E., "Microgrids control: Ac or dc, that is not the question," *EPJ Web Conf.*, vol. 310, p. 00015, 2024.
- [21] M. Huang, L. Ding, W. Li, C.-Y. Chen, and Z. Liu, "Distributed observer-based  $h_\infty$  fault-tolerant control for DC microgrids with sensor fault," *IEEE Transactions on Circuits and Systems I: Regular Papers*, vol. 68, no. 4, pp. 1659–1670, 2021.
- [22] W. Syed, "Dc microgrid model, constraint and control parameters (v1.0.1)," 2026, dataset. [Online]. Available: <https://doi.org/10.5281/zenodo.18529516>
- [23] G. Qu and N. Li, "On the exponential stability of primal-dual gradient dynamics," *arXiv preprint*, 2018. [Online]. Available: <https://arxiv.org/abs/1803.01825>
- [24] R. A. Horn and C. R. Johnson, *Matrix analysis*. Cambridge university press, 2012.

## APPENDIX

### A. Proof of Lemma 2

To prove Lemma 2, we follow a proof strategy similar to the inequality-only case in [11]. To improve readability, key facts relevant for proving Lemma 2 are presented in the form of preliminary propositions, after which we give a re-statement of Lemma 2 and present its proof.

*Proposition 1:* Let  $P_2$  be defined in (20). Let  $\epsilon \in (0, 1)$  and let  $R$  be the stacked constraint matrix defined in (10). Suppose that  $RR^\top \preceq \kappa_2 \mathbf{I}$  holds (Assumption 5). If  $c$  is such that (21b) holds, i.e.,

$$c \geq \begin{cases} \eta \sqrt{\frac{\kappa_2}{(\eta - \epsilon)(1 - \epsilon)}}, & \eta \geq 1, \\ \sqrt{\frac{\eta \kappa_2}{(1 - \epsilon)(1 - \eta\epsilon)}}, & 0 < \eta < 1, \end{cases}$$

then

$$P_2 \succeq \epsilon c \min(\eta, 1) \mathbf{I}, \quad (36)$$

and, in particular,  $P_2$  is positive definite.  $\square$

**Proof.** Consider

$$\tilde{P}_2 := P_2 - \epsilon c \min(\eta, 1) \mathbf{I}.$$

Using the stacked matrix  $R$ , the matrix  $P_2$  in (20) can be written as

$$P_2 = \begin{bmatrix} \eta c \mathbf{I} & \eta R^\top \\ \eta R & c \mathbf{I} \end{bmatrix},$$

and hence

$$\tilde{P}_2 = \begin{bmatrix} c(\eta - \epsilon \min(\eta, 1)) \mathbf{I} & \eta R^\top \\ \eta R & c(1 - \epsilon \min(\eta, 1)) \mathbf{I} \end{bmatrix}.$$

We show  $\tilde{P}_2 \succeq 0$  by a Schur-complement argument.

*Case 1:*  $\eta \geq 1$ . Then  $\min(\eta, 1) = 1$  and

$$\tilde{P}_2 = \begin{bmatrix} c(\eta - \epsilon) \mathbf{I} & \eta R^\top \\ \eta R & c(1 - \epsilon) \mathbf{I} \end{bmatrix}.$$

Since  $\eta > \epsilon$ , the leading block  $c(\eta - \epsilon) \mathbf{I} \succ 0$ . By the Schur complement,  $\tilde{P}_2 \succeq 0$  is implied by

$$c(1 - \epsilon) \mathbf{I} - \frac{\eta^2}{c(\eta - \epsilon)} R R^\top \succeq 0.$$

Using  $RR^\top \preceq \kappa_2 \mathbf{I}$ , it is sufficient that

$$\begin{aligned} c(1 - \epsilon) - \frac{\eta^2}{c(\eta - \epsilon)} \kappa_2 &\geq 0 \\ \iff c^2(1 - \epsilon)(\eta - \epsilon) &\geq \eta^2 \kappa_2. \end{aligned} \quad (37)$$

*Case 2:*  $0 < \eta < 1$ . Then  $\min(\eta, 1) = \eta$  and

$$\tilde{P}_2 = \begin{bmatrix} \eta c(1 - \epsilon) \mathbf{I} & \eta R^\top \\ \eta R & c(1 - \eta\epsilon) \mathbf{I} \end{bmatrix}.$$

Since  $\epsilon \in (0, 1)$ , the leading block  $\eta c(1 - \epsilon) \mathbf{I} \succ 0$ . By the Schur complement,  $\tilde{P}_2 \succeq 0$  is implied by

$$c(1 - \eta\epsilon) \mathbf{I} - \frac{\eta}{c(1 - \epsilon)} R R^\top \succeq 0.$$

Using  $RR^\top \preceq \kappa_2 \mathbf{I}$ , it is sufficient that

$$\begin{aligned} c(1 - \eta\epsilon) - \frac{\eta}{c(1 - \epsilon)} \kappa_2 &\geq 0 \\ \iff c^2(1 - \epsilon)(1 - \eta\epsilon) &\geq \eta\kappa_2. \end{aligned} \quad (38)$$

Then, if  $c$  is as in the Proposition's statement, we can see directly that (37) holds in Case 1 and (38) holds in Case 2, and hence  $\tilde{P}_2 \succeq 0$ . Therefore,  $P_2 \succeq \epsilon c \min(\eta, 1) \mathbf{I}$ , which proves (67). Since  $\epsilon c \min(\eta, 1) > 0$ , this further implies  $P_2 \succ 0$ .  $\blacksquare$

*Proposition 2:* Let

$$\phi_i := \nu_{\text{ineq},i} + \rho (R_{\text{ineq}} \xi - h)_i. \quad (39)$$

Then, there exists a symmetric matrix  $H(\xi) \in \mathbb{R}^{n_\xi \times n_\xi}$  and functions  $\phi_i \mapsto \gamma_i(\phi_i)$  satisfying, for  $i = 1, 2, \dots, n_{\text{ineq}}$ ,

$$\gamma_i(\phi_i) \in [0, 1], \quad (40)$$

such that the shifted dynamics (error dynamics) of the Aug-PDGD (19) can be written as

$$\dot{\tilde{\theta}} = F(\theta)\tilde{\theta} + B_{\text{pd}}\tilde{v}_{\text{pd}}, \quad (41)$$

with

$$F(\theta) = \begin{bmatrix} -H(\xi) - \rho R_{\text{ineq}}^\top \Gamma(\phi) R_{\text{ineq}} & -R_{\text{eq}}^\top & -R_{\text{ineq}}^\top \Gamma(\phi) \\ \eta R_{\text{eq}} & \mathbf{0} & \mathbf{0} \\ \eta \Gamma(\phi) R_{\text{ineq}} & \mathbf{0} & \frac{\eta}{\rho} (\Gamma(\phi) - \mathbf{I}) \end{bmatrix} \quad (42a)$$

and

$$\Gamma(\phi) := \text{diag}(\gamma_1(\phi_1), \dots, \gamma_{n_{\text{ineq}}}(\phi_{n_{\text{ineq}}})). \quad (42b)$$

Moreover, the matrix  $H(\xi)$  satisfies

$$\mu \mathbf{I} \leq H(\xi) \leq \ell \mathbf{I}, \quad (43)$$

where  $0 < \mu \leq \ell$  are as in Assumption 4.  $\square$

**Proof.** Recall that  $\bar{\theta} = (\bar{\xi}, \bar{v}_{\text{eq}}, \bar{v}_{\text{ineq}})$  is the unique solution of the KKT conditions (12), and is at the same time the unique equilibrium of the Aug-PDGD (19) when  $v_{\text{pd}} = \bar{v}_{\text{pd}} = \mathbf{0}$ . By defining  $\tilde{\theta} = \theta - \bar{\theta}$  and  $\tilde{v}_{\text{pd}} = v_{\text{pd}} - \bar{v}_{\text{pd}}$ , it holds that

$$\dot{\tilde{\theta}} = \begin{pmatrix} -(\nabla J(\xi) - \nabla J(\bar{\xi})) - R_{\text{eq}}^\top \tilde{v}_{\text{eq}} - R_{\text{ineq}}^\top (g(\xi, \nu_{\text{ineq}}) - g(\bar{\xi}, \bar{v}_{\text{ineq}})) \\ \eta R_{\text{eq}} \tilde{\xi} \\ \frac{\eta}{\rho} (g(\xi, \nu_{\text{ineq}}) - g(\bar{\xi}, \bar{v}_{\text{ineq}}) - \tilde{v}_{\text{ineq}}) \end{pmatrix} + B_{\text{pd}}\tilde{v}_{\text{pd}}, \quad (44)$$

By Assumption 4 and the mean value theorem, then [23]

$$\nabla J(\xi) - \nabla J(\bar{\xi}) = H(\xi)(\xi - \bar{\xi}), \quad (45)$$

where

$$H(\xi) := \int_0^1 \nabla^2 J(\bar{\xi} + s(\xi - \bar{\xi})) ds.$$

Note already that due to Assumption 4,  $\mu \mathbf{I} \preceq H(\xi) \preceq \ell \mathbf{I}$  for all  $\xi$ , which establishes (43).

Moving on, we focus now on finding an alternative representation for the term  $g(\xi, \nu_{\text{ineq}}) - g(\bar{\xi}, \bar{v}_{\text{ineq}})$  in (44). For that purpose, let us introduce  $\phi_i$  as in (39). Then,  $g(\xi, \nu_{\text{ineq}}) = \max(\nu_{\text{ineq}} + \rho (R_{\text{ineq}} \xi - h), 0)$ , from (17), can be written component-wise as

$$g(\xi, \nu_{\text{ineq}})_i := \max(\phi_i, 0). \quad (46)$$

For brevity, we suppress in the sequel the dependence of  $g_i$  on  $(\xi, \nu_{\text{ineq}})$ . Likewise, define  $\bar{\phi}_i := \bar{v}_{\text{ineq},i} + \rho (R_{\text{ineq}} \bar{\xi} - h)_i$  so that  $\bar{g}_i = \max(\bar{\phi}_i, 0)$ . Then the following identity holds:

$$\max(\phi_i, 0) - \max(\bar{\phi}_i, 0) = \gamma_i(\phi_i) (\phi_i - \bar{\phi}_i),$$

where  $\gamma_i$ , defined as,

$$\gamma_i(\phi_i) := \begin{cases} 1, & \phi_i > 0, \bar{\phi}_i > 0, \\ 0, & \phi_i \leq 0, \bar{\phi}_i \leq 0, \\ \frac{\phi_i}{\phi_i - \bar{\phi}_i}, & \phi_i > 0, \bar{\phi}_i \leq 0, \\ \frac{-\bar{\phi}_i}{\phi_i - \bar{\phi}_i}, & \phi_i \leq 0, \bar{\phi}_i > 0, \end{cases} \quad (47)$$

can be directly shown to satisfy  $\gamma_i(\phi_i) \in [0, 1]$ . Moreover, by noting that

$$\phi_i - \bar{\phi}_i = \tilde{\nu}_{\text{ineq},i} + \rho (R_{\text{ineq}} \tilde{\xi})_i,$$

we obtain that

$$g_i - \bar{g}_i = \gamma_i(\phi_i) \left( \tilde{\nu}_{\text{ineq},i} + \rho (R_{\text{ineq}} \tilde{\xi})_i \right). \quad (48)$$

Now define the diagonal matrix

$$\Gamma(\phi) := \text{diag}(\gamma_1(\phi_1), \dots, \gamma_{n_{\text{ineq}}}(\phi_{n_{\text{ineq}}})).$$

Then,

$$g - \bar{g} = \Gamma(\phi) \tilde{\nu}_{\text{ineq}} + \rho \Gamma(\phi) R_{\text{ineq}} \tilde{\xi} \quad (49)$$

Using (45) and (49) we can rewrite (44) as

$$\dot{\tilde{\theta}} = \begin{bmatrix} -H(\xi) - \rho R_{\text{ineq}}^\top \Gamma(\phi) R_{\text{ineq}} & -R_{\text{eq}}^\top & -R_{\text{ineq}}^\top \Gamma(\phi) \\ \eta R_{\text{eq}} & \mathbf{0} & \mathbf{0} \\ \eta \Gamma(\phi) R_{\text{ineq}} & \mathbf{0} & \frac{\eta}{\rho} (\Gamma(\phi) - \mathbf{I}) \end{bmatrix} \begin{bmatrix} \tilde{\xi} \\ \tilde{\nu}_{\text{eq}} \\ \tilde{\nu}_{\text{ineq}} \end{bmatrix} + B_{\text{pd}} \tilde{v}_{\text{pd}}. \quad (50)$$

*Proposition 3:* Recall the matrix  $P_2 = \begin{bmatrix} \eta c \mathbf{I} & \eta R_{\text{eq}}^\top & \eta R_{\text{ineq}}^\top \\ \eta R_{\text{eq}} & c \mathbf{I} & \mathbf{0} \\ \eta R_{\text{ineq}} & \mathbf{0} & c \mathbf{I} \end{bmatrix}$  from (20), the matrix  $F(\theta)$  from (42a), and  $\tau_2 = \frac{\eta \kappa_1}{2c}$  from (23). Then,

$$\begin{aligned} Q &:= -F(\theta)^\top P_2 - P_2 F(\theta) - \tau_2 P_2 \\ &= \begin{bmatrix} 2\eta c H + 2\eta c \rho R^\top \Gamma_2 R - 2\eta^2 R^\top \Gamma_1 R - \frac{\eta^2 \kappa_1}{2} \mathbf{I} & \eta \left( H + \rho R^\top \Gamma_2 R - \frac{\eta \kappa_1}{2c} \mathbf{I} \right) R^\top + \eta \frac{\eta}{\rho} R^\top (\mathbf{I} - \Gamma_1) \\ *^\top & \eta (\Gamma_1 R R^\top + R R^\top \Gamma_1) + \frac{2\eta c}{\rho} (\mathbf{I} - \Gamma_1) - \frac{\eta \kappa_1}{2} \mathbf{I} \end{bmatrix}. \end{aligned} \quad (51)$$

□

**Proof.** We begin by writing  $F(\theta)$  as a 2-by-2 block matrix. For that purpose, let us define

$$\Gamma_1(\phi) = \text{blkdiag}(\mathbf{I}, \Gamma(\phi)), \quad \Gamma_2(\phi) = \text{blkdiag}(\mathbf{0}, \Gamma(\phi)), \quad (52)$$

where we recall that  $\Gamma$  is the diagonal function matrix defined in (42b), with  $\phi$  defined by components in (39). Then,

$$F(\theta) = \begin{bmatrix} -H & -\rho R^\top \Gamma_2 R & -R^\top \Gamma_1 \\ \eta \Gamma_1 R & \eta \left( \Gamma_1 - \mathbf{I} \right) \end{bmatrix},$$

where  $R$  is defined as in (10). Similarly, for the (symmetric, constant) matrix  $P_2$  it is possible to write the following representation:

$$P_2 = \begin{bmatrix} \eta c \mathbf{I} & \eta R^\top \\ \eta R & c \mathbf{I} \end{bmatrix}.$$

It follows that

$$\begin{aligned}
P_2 F(\theta) &= \begin{bmatrix} \eta c \mathbf{I} & \eta R^\top \\ \eta R & c \mathbf{I} \end{bmatrix} \begin{bmatrix} -H - \rho R^\top \Gamma_2 R & -R^\top \Gamma_1 \\ \eta \Gamma_1 R & \frac{\eta}{\rho} (\Gamma_1 - \mathbf{I}) \end{bmatrix} \\
&= \begin{bmatrix} -\eta c H - \eta c \rho R^\top \Gamma_2 R + \eta^2 R^\top \Gamma_1 R & -\eta c R^\top \Gamma_1 + \frac{\eta^2}{\rho} R^\top (\Gamma_1 - \mathbf{I}) \\ -\eta R H - \eta \rho R R^\top \Gamma_2 R + c \eta \Gamma_1 R & -\eta R R^\top \Gamma_1 + \frac{c \eta}{\rho} (\Gamma_1 - \mathbf{I}) \end{bmatrix} \tag{53}
\end{aligned}$$

and

$$\begin{aligned}
F^\top(\theta) P_2 &= \begin{bmatrix} -H^\top - \rho R^\top \Gamma_2 R & \eta R^\top \Gamma_1 \\ -\Gamma_1 R & \frac{\eta}{\rho} (\Gamma_1 - \mathbf{I}) \end{bmatrix} \begin{bmatrix} \eta c \mathbf{I} & \eta R^\top \\ \eta R & c \mathbf{I} \end{bmatrix} \\
&= \begin{bmatrix} -\eta c H - \eta c \rho R^\top \Gamma_2 R + \eta^2 R^\top \Gamma_1 R & -\eta H R^\top - \eta \rho R^\top \Gamma_2 R R^\top + c \eta R^\top \Gamma_1 \\ -\eta c \Gamma_1 R + \frac{\eta^2}{\rho} (\Gamma_1 - \mathbf{I}) R & -\eta \Gamma_1 R R^\top + \frac{c \eta}{\rho} (\Gamma_1 - \mathbf{I}) \end{bmatrix} \tag{54}
\end{aligned}$$

Consequently,

$$\begin{aligned}
Q &= -F^\top(\theta) P_2 - P_2 F(\theta) - \tau_2 P_2 \\
&= - \begin{bmatrix} -\eta c H - \eta c \rho R^\top \Gamma_2 R + \eta^2 R^\top \Gamma_1 R & -\eta H R^\top - \eta \rho R^\top \Gamma_2 R R^\top + c \eta R^\top \Gamma_1 \\ -\eta c \Gamma_1 R + \frac{\eta^2}{\rho} (\Gamma_1 - \mathbf{I}) R & -\eta \Gamma_1 R R^\top + \frac{c \eta}{\rho} (\Gamma_1 - \mathbf{I}) \end{bmatrix} \\
&\quad - \begin{bmatrix} -\eta c H - \eta c \rho R^\top \Gamma_2 R + \eta^2 R^\top \Gamma_1 R & -\eta c R^\top \Gamma_1 + \frac{\eta^2}{\rho} R^\top (\Gamma_1 - \mathbf{I}) \\ -\eta R H - \eta \rho R R^\top \Gamma_2 R + c \eta \Gamma_1 R & -\eta R R^\top \Gamma_1 + \frac{c \eta}{\rho} (\Gamma_1 - \mathbf{I}) \end{bmatrix} \\
&\quad - \underbrace{\frac{\eta \kappa_1}{2c} \begin{bmatrix} \eta c \mathbf{I} & \eta R^\top \\ \eta R & c \mathbf{I} \end{bmatrix}}_{\tau_2} \\
&= \begin{bmatrix} 2\eta c H + 2\eta c \rho R^\top \Gamma_2 R - 2\eta^2 R^\top \Gamma_1 R - \frac{\eta^2 \kappa_1}{2} \mathbf{I} & \eta \left( H + \rho R^\top \Gamma_2 R - \frac{\eta \kappa_1}{2c} \mathbf{I} \right) R^\top + \eta \frac{\eta}{\rho} R^\top (\mathbf{I} - \Gamma_1) \\ *^\top & \eta (\Gamma_1 R R^\top + R R^\top \Gamma_1) + \frac{2\eta c}{\rho} (\mathbf{I} - \Gamma_1) - \frac{\eta \kappa_1}{2} \mathbf{I} \end{bmatrix}, \tag{55}
\end{aligned}$$

as stated.  $\blacksquare$

The following proposition is key to establish that  $Q$  in (51) is positive semi-definite.

*Proposition 4:* ([11, Lemma 6]) Let  $c$  be chosen as in (21). Recall the diagonal function matrix  $\Gamma_1$  from (52) (see also (40)). Then, for  $\eta > 0$  and  $\rho > 0$  as introduced in (15) and (14), respectively, the following inequality holds:

$$\eta (\Gamma_1 R R^\top + R R^\top \Gamma_1) + \frac{2\eta c}{\rho} (\mathbf{I} - \Gamma_1) \succeq \frac{3}{2} \eta R R^\top, \tag{56}$$

where  $R$  is defined in (10).  $\square$

**Proof.** Let us denote by  $d_{1,1}, d_{1,2}, \dots, d_{1,n_c}$  the main diagonal elements of  $\Gamma_1 = \text{blkdiag}(\mathbf{I}, \Gamma(\phi))$ , with  $\Gamma$  in (42b) and  $\phi$  defined by components in (39), and let us refer by  $M(d_{1,1}, \dots, d_{1,n_c})$  to the matrix in the left-hand side of (56):

$$M(d_{1,1}, \dots, d_{1,n_c}) := \eta (\Gamma_1 R R^\top + R R^\top \Gamma_1) + \frac{2\eta c}{\rho} (\mathbf{I} - \Gamma_1), \tag{57}$$

where  $\eta > 0$ ,  $\rho > 0$  and  $c > 0$  are fixed constants. Now, since  $\Gamma_1$  is diagonal, it holds that each entry of  $\Gamma_1 R R^\top$ ,  $R R^\top \Gamma_1$ , and  $\mathbf{I} - \Gamma_1$  depends linearly on each  $d_{1,i}$ . Then, for fixed  $R, \eta, c$  and  $\rho$ , the mapping  $(d_{1,1}, \dots, d_{1,n_c}) \mapsto M_\gamma(d_{1,1}, \dots, d_{1,n_c})$  is affine in each variable  $d_{1,i}$ . Moreover, note that  $d_{1,i}$  is either 1, or equal to some function  $\gamma_j(\phi_j)$  introduced in (47). Then, each  $d_{1,i}$  satisfies

$$d_{1,i} \in [0, 1]. \tag{58}$$

These facts will be exploited to establish the following inequality:

$$M(d_{1,1}, \dots, d_{1,n_c}) \succeq \frac{3}{2} \eta R R^\top, \quad \forall d_{1,i} \in [0, 1], \tag{59}$$

from which (56) would directly follow. For that purpose, note that since  $M$  is affine in  $d_{1,1}, \dots, d_{1,n_c}$ , and the unit cube  $[0, 1]^{n_c}$  is a convex polytope, it holds that  $M$  can be written as a convex combination of  $2^{n_c}$  constant matrices obtained by evaluating  $M$  at each vertex  $b = (b_1, \dots, b_{n_c}) \in \{0, 1\}^{n_c}$  of  $[0, 1]^{n_c}$ . That is,

$$M(d_{1,1}, \dots, b_{1,n_c}) = \sum_{b \in \{0,1\}^{n_c}} \alpha_b(d_{1,1}, \dots, d_{1,n_c}) M(b_1, \dots, b_{n_c}), \quad (60a)$$

with coefficients  $\alpha_b$  given by

$$\alpha_b(d_{1,1}, \dots, d_{1,n_c}) := \prod_{i:b_i=1} d_{1,i} \prod_{i:b_i=0} (1 - d_{1,i}) \quad (60b)$$

and satisfying

$$\alpha_b(d_{1,1}, \dots, d_{1,n_c}) \geq 0, \quad \sum_{b \in \{0,1\}^{n_c}} \alpha_b(d_{1,1}, \dots, d_{1,n_c}) = 1. \quad (60c)$$

Then, to establish (59), it suffices to show that

$$M(b_1, \dots, b_{n_c}) \succeq \frac{3}{2} \eta R R^\top \quad \forall b \in \{0, 1\}^{n_c}. \quad (61)$$

To that end, let  $b \in \{0, 1\}^{n_c}$  be arbitrary, and let us assume that each of the first  $k$  main diagonal entries of  $\Gamma_1$  are equal to one, and that the remaining ones are zero<sup>10</sup>. Then, we can write the product  $R R^\top$  as follows:

$$R R^\top = \begin{bmatrix} \Sigma_1 & \Sigma_3 \\ \Sigma_3^\top & \Sigma_2 \end{bmatrix}, \quad (62)$$

where  $\Sigma_1 \in \mathbb{R}^{k \times k}$ ,  $\Sigma_2 \in \mathbb{R}^{(n_c-k) \times (n_c-k)}$ ,  $\Sigma_3 \in \mathbb{R}^{k \times (n_c-k)}$ . It follows that

$$\Gamma_1 R R^\top = \begin{bmatrix} \Sigma_1 & \Sigma_3 \\ 0 & 0 \end{bmatrix}, \quad R R^\top \Gamma_1 = \begin{bmatrix} \Sigma_1 & 0 \\ \Sigma_3^\top & 0 \end{bmatrix}, \quad \mathbf{I} - \Gamma_1 = \begin{bmatrix} 0 & 0 \\ 0 & \mathbf{I}_{n_c-k} \end{bmatrix}.$$

Then,

$$\begin{aligned} M(b_1, \dots, b_{n_c}) &= M(1, \dots, 1_k, 0, \dots, 0) \\ &= \eta \left( \begin{bmatrix} \mathbf{I}_k & 0 \\ 0 & \mathbf{0}_{n_c-k} \end{bmatrix} \begin{bmatrix} \Sigma_1 & \Sigma_3 \\ \Sigma_3^\top & \Sigma_2 \end{bmatrix} + \begin{bmatrix} \Sigma_1 & \Sigma_3 \\ \Sigma_3^\top & \Sigma_2 \end{bmatrix} \begin{bmatrix} \mathbf{I}_k & 0 \\ 0 & \mathbf{0}_{n_c-k} \end{bmatrix} \right) + \frac{2\eta c}{\rho} \left( \begin{bmatrix} \mathbf{I}_k & 0 \\ 0 & \mathbf{I}_{n_c-k} \end{bmatrix} - \begin{bmatrix} \mathbf{I}_k & 0 \\ 0 & \mathbf{0}_{n_c-k} \end{bmatrix} \right) \\ &= \eta \left( \begin{bmatrix} \Sigma_1 & \Sigma_3 \\ 0 & 0 \end{bmatrix} + \begin{bmatrix} \Sigma_1 & 0 \\ \Sigma_3^\top & 0 \end{bmatrix} \right) + \frac{2\eta c}{\rho} \begin{bmatrix} \mathbf{0}_k & 0 \\ 0 & \mathbf{I}_{n_c-k} \end{bmatrix} \\ &= \begin{bmatrix} 2\eta \Sigma_1 & \eta \Sigma_3 \\ \eta \Sigma_3^\top & \frac{2\eta c}{\rho} \mathbf{I}_{n_c-k} \end{bmatrix}. \end{aligned} \quad (63)$$

Consequently, (61) is equivalent to the following expression:

$$\frac{\eta}{2} \begin{bmatrix} \Sigma_1 & -\Sigma_3 \\ -\Sigma_3^\top & \frac{4c}{\rho} \mathbf{I}_{n_c-k} - 3\Sigma_2 \end{bmatrix} \succeq \mathbf{0}. \quad (64)$$

From Assumption 5,  $R R^\top \preceq \kappa_2 \mathbf{I}$ , where  $\kappa_2$  is in (11). Considering (62), it holds that  $\Sigma_2 \preceq \kappa_2 \mathbf{I}_{n_c-k}$ . Moreover, since  $c \geq \kappa_2 \rho$  (see (21c)), it follows that the sub-block  $\frac{4c}{\rho} \mathbf{I}_{n_c-k} - 3\Sigma_2$  satisfies the following

$$\frac{4c}{\rho} \mathbf{I}_{n_c-k} - 3\Sigma_2 \succeq \Sigma_2. \quad (65)$$

Then, the matrix in the left-hand side of (64) can be lower bounded as follows:

$$\frac{\eta}{2} \begin{bmatrix} \Sigma_1 & -\Sigma_3 \\ -\Sigma_3^\top & \frac{4c}{\rho} \mathbf{I}_{n_c-k} - 3\Sigma_2 \end{bmatrix} \succeq \frac{\eta}{2} \begin{bmatrix} \Sigma_1 & -\Sigma_3 \\ -\Sigma_3^\top & \Sigma_2 \end{bmatrix}. \quad (66)$$

<sup>10</sup>This assumption is without loss of generality. Indeed, let  $b \in \{0, 1\}^{n_c}$  be arbitrary, and define  $k = \sum_i b_i$ . Now, choose a permutation matrix [24]  $P$  such that  $P \Gamma_1 P^\top = \Gamma_{1,k} := \text{diag}(1, \dots, 1_k, 0, \dots, 0)$ . If we define  $\widetilde{R} R^\top := P R R^\top P^\top$  and use the identity  $P^\top P = \mathbf{I}$ , then we obtain that  $P(\Gamma_1 R R^\top)P^\top = (P\Gamma_1 P^\top)(P R R^\top P^\top) = \widetilde{\Gamma}_{1,k} \widetilde{R} R^\top$ ,  $P(R R^\top \Gamma_1)P^\top = \widetilde{R} R^\top \widetilde{\Gamma}_{1,k}$ , and  $P(\mathbf{I} - \Gamma_1)P^\top = \mathbf{I} - \widetilde{\Gamma}_{1,k}$ . Then, the permuted matrix  $\widetilde{M}(b) := P M(b) P^\top$  satisfies  $\widetilde{M}(b) = \eta(\widetilde{\Gamma}_{1,k} \widetilde{R} R^\top + \widetilde{R} R^\top \widetilde{\Gamma}_{1,k}) + \frac{2\eta c}{\rho}(\mathbf{I} - \widetilde{\Gamma}_{1,k})$ . Since orthogonal congruence preserves the semi-definiteness order [24], we have that  $M_\gamma(b) \succeq \frac{3}{2} \eta R R^\top$  if and only if  $\widetilde{M} \succeq \frac{3}{2} \eta \widetilde{R} R^\top$ . Hence we may assume without loss of generality that the ones in  $\Gamma_1$  occupy the first  $k$  diagonal entries.

The matrix in the right-hand side of (66) is congruent to  $RR^\top$  with orthogonal matrix  $\begin{bmatrix} \mathbf{I}_k & 0 \\ 0 & -\mathbf{I}_{n_c-k} \end{bmatrix}$ . From Assumption 5,  $RR^\top$  is positive definite. Therefore, (64) and consequently (61), which in chain implies (59) and (56), hold true. This concludes the proof.  $\blacksquare$

*Lemma 2:* Fix  $\eta > 0$  and  $\epsilon \in (0, 1)$ , let Assumptions 4 and 5 hold, and fix  $c > 0$  according to (21). Then,  $P_2$  in (20) satisfies

$$P_2 \succeq \epsilon c \min(\eta, 1) \mathbf{I}. \quad (67)$$

Moreover, the Aug-PDGD (19) is strictly shifted-passive with quadratic storage function  $S_c(\tilde{\theta}) = \tilde{\theta}^\top P_2 \tilde{\theta}$  and with respect to the input-output pair  $(\tilde{v}_{\text{pd}}, 2 B_{\text{pd}}^\top P_2 \tilde{\theta})$ . In particular, it holds that

$$\dot{S}_c \leq -\tau_2 \tilde{\theta}^\top P_2 \tilde{\theta} + 2 \tilde{\theta}^\top P_2 B_{\text{pd}} \tilde{v}_{\text{pd}}$$

along any system trajectory, with

$$\tau_2 := \frac{\eta \kappa_1}{2c}.$$

$\square$

**Proof.** Recall from Proposition 1 that  $P_2 \succ \mathbf{0}$ . Moreover, by Proposition 2, the Aug-PDGD (19) is equivalent to its shifted dynamics (41). Then, along any of its solutions the time derivative of  $S_c$  satisfies the following:

$$\begin{aligned} \dot{S}_c &= \dot{\tilde{\theta}}^\top P_2 \tilde{\theta} + \tilde{\theta}^\top P_2 \dot{\tilde{\theta}} \\ &= \tilde{\theta}^\top (F^\top P_2 + P_2 F) \tilde{\theta} + 2 \tilde{\theta}^\top P_2 B_{\text{pd}} \tilde{v}_{\text{pd}}, \end{aligned} \quad (68)$$

where for simplicity we have removed the dependency of  $F$  with respect to  $\theta$  (see (42a)). To show shifted-passivity, it suffices to verify that

$$F^\top P_2 + P_2 F \preceq -\tau_2 P_2,$$

or, equivalently, that

$$Q = -F^\top P_2 - P_2 F - \tau_2 P_2 \succeq \mathbf{0}.$$

We recall from Proposition 3 that

$$\begin{aligned} Q &= \begin{bmatrix} 2\eta c H + 2\eta c \rho R^\top \Gamma_2 R - 2\eta^2 R^\top \Gamma_1 R - \frac{\eta^2 \kappa_1}{2} \mathbf{I} & \eta \left( H + \rho R^\top \Gamma_2 R - \frac{\eta \kappa_1}{2c} \mathbf{I} \right) R^\top + \eta \frac{\eta}{\rho} R^\top (\mathbf{I} - \Gamma_1) \\ *^\top & \eta (\Gamma_1 R R^\top + R R^\top \Gamma_1) + \frac{2\eta c}{\rho} (\mathbf{I} - \Gamma_1) - \frac{\eta \kappa_1}{2} \mathbf{I} \end{bmatrix} \\ &=: \begin{bmatrix} Q_1 & Q_3 \\ Q_3^\top & Q_2 \end{bmatrix}. \end{aligned}$$

By the Schur complement, to show that  $Q \succeq \mathbf{0}$  it suffices to verify that

$$Q_2 \succ \mathbf{0}, \quad Q_1 - Q_3 Q_2^{-1} Q_3^\top \succeq \mathbf{0}.$$

From Proposition 4, the condition  $c \geq \kappa_2 \rho$  is sufficient for ensuring that

$$Q_2 \succeq \frac{3}{2} \eta R R^\top - \frac{\eta \kappa_1}{2} \mathbf{I}. \quad (69)$$

Since  $R R^\top \succeq \kappa_1 \mathbf{I}$  due to Assumption 5, it holds that  $Q_2 \succ \mathbf{0}$ .

We proceed to show that  $Q_1 - Q_3 Q_2^{-1} Q_3^\top \succeq \mathbf{0}$ . To establish this, we will first show that the following holds:

$$Q_1 \succeq 2\eta c H - h_1(c) \mathbf{I} \quad (70a)$$

$$Q_3 Q_2^{-1} Q_3^\top \preceq \eta \ell H + (h_2(c) + h_3(c) + h_4(c)) \mathbf{I}, \quad (70b)$$

where

$$h_1 = 2\eta^2 \kappa_2 + \frac{\eta^2 \kappa_1}{2}, \quad (70c)$$

$$h_2(c) = 2\eta \ell (\rho \kappa_2 + \frac{\eta \kappa_1}{2c}) + \eta (\rho \kappa_2 + \frac{\eta \kappa_1}{2c})^2, \quad (70d)$$

$$h_3(c) = \frac{2\eta^2}{\rho} \left( \ell + \rho \kappa_2 + \frac{\eta \kappa_1}{2c} \right) \frac{\kappa_2}{\kappa_1}, \quad (70e)$$

$$h_4 = \eta^3 \rho^{-2} \frac{\kappa_2}{\kappa_1}. \quad (70f)$$

Before proceeding, we find it convenient to recall the following facts. The matrix  $\Gamma_1$ , defined in (52), satisfies  $\Gamma_1 \preceq \mathbf{I}$ . The matrix  $H$ , defined in Proposition 2, is symmetric positive-definite and satisfies  $\mu\mathbf{I} \preceq H \preceq \ell\mathbf{I}$ . The matrix  $R$ , introduced in (9c), is such that  $\kappa_1\mathbf{I} \preceq RR^\top \preceq \kappa_2\mathbf{I}$ .

**Let us continue then by verifying** (70a). Note directly that

$$Q_1 = 2\eta c H + 2\eta c \rho R^\top \Gamma_2 R - 2\eta^2 R^\top \Gamma_1 R - \frac{\eta^2 \kappa_1}{2} \mathbf{I} \succeq 2\eta c H - 2\eta^2 R^\top \Gamma_1 R - \frac{\eta^2 \kappa_1}{2} \mathbf{I}. \quad (71)$$

Since  $\Gamma_1 \preceq \mathbf{I}$  and  $R^\top R \preceq \kappa_2\mathbf{I}$ , then (70a) is verified.

**Next, we show that** (70b) **holds**. Let us write  $Q_3$  as follows

$$Q_3 = \eta Q_{3,a} R^\top + \eta Q_{3,b}, \quad (72)$$

where

$$Q_{3,a} := H + \rho R^\top \Gamma_2 R - \frac{\eta \kappa_1}{2c} \mathbf{I}, \quad Q_{3,b} := \frac{\eta}{\rho} R^\top (\mathbf{I} - \Gamma_1). \quad (73)$$

Now, note from (69) that  $Q_2 \succeq \eta RR^\top$  implies that  $Q_2^{-1} \preceq \frac{1}{\eta}(RR^\top)^{-1}$  (recall that  $RR^\top$  is positive-definite and hence invertible). Then the following holds:

$$\begin{aligned} Q_3 Q_2^{-1} Q_3^\top &\preceq Q_3 \left( \frac{1}{\eta} (RR^\top)^{-1} \right) Q_3^\top \\ &= (\eta Q_{3,a} R^\top + \eta Q_{3,b}) \left( \frac{1}{\eta} (RR^\top)^{-1} \right) (\eta R Q_{3,a}^\top + \eta Q_{3,b}^\top) \\ &= \eta Q_{3,a} R^\top (RR^\top)^{-1} R Q_{3,a}^\top + 2\text{symm}\{\eta Q_{3,a} R^\top (RR^\top)^{-1} Q_{3,b}^\top\} + \eta Q_{3,b} (RR^\top)^{-1} Q_{3,b}^\top. \end{aligned} \quad (74)$$

Since for any symmetric matrix  $M$ ,  $M \preceq \|M\|\mathbf{I}$ , and  $R^\top (RR^\top)^{-1} R \preceq \mathbf{I}$ , then the right-hand side of (74) satisfies the following:

$$\begin{aligned} &\eta Q_{3,a} R^\top (RR^\top)^{-1} R Q_{3,a}^\top + 2\text{symm}\{\eta Q_{3,a} R^\top (RR^\top)^{-1} Q_{3,b}^\top\} + \eta Q_{3,b} (RR^\top)^{-1} Q_{3,b}^\top \\ &\preceq \eta Q_{3,a} Q_{3,a}^\top + 2\eta \|Q_{3,a} R^\top (RR^\top)^{-1} Q_{3,b}^\top\| \mathbf{I} + \eta \|Q_{3,b} (RR^\top)^{-1} Q_{3,b}^\top\| \mathbf{I}. \end{aligned} \quad (75)$$

Let us develop upper bounds for each of the terms in the right-hand side of (75). We begin with  $\eta Q_{3,a} Q_{3,a}^\top$ :

$$\begin{aligned} \eta Q_{3,a} Q_{3,a}^\top &= \eta \left( H + \rho R^\top \Gamma_2 R - \frac{\eta \kappa_1}{2c} \mathbf{I} \right) \left( H + \rho R^\top \Gamma_2 R - \frac{\eta \kappa_1}{2c} \mathbf{I} \right) \\ &= \eta \left( H^2 + 2\text{symm}\{H(\rho R^\top \Gamma_2 R - \frac{\eta \kappa_1}{2c} \mathbf{I})\} + (\rho R^\top \Gamma_2 R - \frac{\eta \kappa_1}{2c} \mathbf{I})^2 \right) \\ &\preceq \eta H^2 + 2\eta \|H\| \|\rho R^\top \Gamma_2 R - \frac{\eta \kappa_1}{2c} \mathbf{I}\| \mathbf{I} + \eta \|\rho R^\top \Gamma_2 R - \frac{\eta \kappa_1}{2c} \mathbf{I}\|^2 \mathbf{I} \\ &\preceq \eta \ell H + \underbrace{\left( 2\eta \ell (\rho \kappa_2 + \frac{\eta \kappa_1}{2c}) + \eta (\rho \kappa_2 + \frac{\eta \kappa_1}{2c})^2 \right)}_{h_2(c)} \mathbf{I} \\ &= \eta \ell H + h_2(c) \mathbf{I}. \end{aligned} \quad (76)$$

We proceed analogously with the second term and third terms in the right-hand side of (75). For the second term, using sub-multiplicativity, we have that

$$\begin{aligned} 2\eta \|Q_{3,a} R^\top (RR^\top)^{-1} Q_{3,b}^\top\| \mathbf{I} &\preceq 2\eta \|Q_{3,a}\| \|R^\top\| \| (RR^\top)^{-1} \| \|Q_{3,b}^\top\| \mathbf{I} \\ &= 2\eta \left\| H + \rho R^\top \Gamma_2 R - \frac{\eta \kappa_1}{2c} \mathbf{I} \right\| \|R^\top\| \| (RR^\top)^{-1} \| \left\| \frac{\eta}{\rho} (\mathbf{I} - \Gamma_1) R \right\| \mathbf{I} \\ &\preceq 2\eta \left( \|H\| + \rho \|R^\top \Gamma_2 R\| + \frac{\eta \kappa_1}{2c} \|\mathbf{I}\| \right) \|R^\top\| \| (RR^\top)^{-1} \| \left\| \frac{\eta}{\rho} (\mathbf{I} - \Gamma_1) R \right\| \mathbf{I} \end{aligned} \quad (77)$$

Since (43) implies  $\|H\| \leq \ell$ , (11) implies  $\|R^\top R\| \leq \kappa_2$ ,  $\|(R^\top R)^{-1}\| \leq \kappa_1$ , and  $\|R\| = \|R^\top\| \leq \sqrt{\kappa_2}$ , and (52) implies  $\|\Gamma_1\| \leq 1$  and  $\|\Gamma_2\| \leq 1$ , then,

$$\begin{aligned} 2\eta \|Q_{3,a} R^\top (RR^\top)^{-1} Q_{3,b}^\top\| \mathbf{I} &\preceq 2\eta \left( \ell + \rho \kappa_2 + \frac{\eta \kappa_1}{2c} \right) \left( \frac{\sqrt{\kappa_2}}{\kappa_1} \right) \left( \frac{\eta \sqrt{\kappa_2}}{\rho} \right) \mathbf{I} \\ &\preceq \left( \frac{2\eta^2}{\rho} \left( \ell + \rho \kappa_2 + \frac{\eta \kappa_1}{2c} \right) \frac{\kappa_2}{\kappa_1} \right) \mathbf{I} \\ &= h_3(c) \mathbf{I}. \end{aligned} \quad (78)$$

We proceed analogously with the third term, to obtain:

$$\begin{aligned}
\eta \|Q_{3,b}(RR^\top)^{-1}Q_{3,b}^\top\| \mathbf{I} &\preceq \eta \|Q_{3,b}\| \|(RR^\top)^{-1}\| \|Q_{3,b}^\top\| \mathbf{I} \\
&= \eta \|Q_{3,b}\|^2 \|(RR^\top)^{-1}\| \mathbf{I} \\
&= \eta \left\| \frac{\eta}{\rho} (\mathbf{I} - \Gamma_1) R \right\|^2 \|(RR^\top)^{-1}\| \mathbf{I} \\
&\preceq \eta \left( \frac{\eta}{\rho} \right)^2 \|\mathbf{I} - \Gamma_1\|^2 \|R\|^2 \|(RR^\top)^{-1}\| \mathbf{I}.
\end{aligned} \tag{79}$$

Since (52) implies  $\|\mathbf{I} - \Gamma_1\| \leq 1$ , (11) implies  $\|R\| \leq \sqrt{\kappa_2}$  and  $\|(R^\top R)^{-1}\| \leq \kappa_1$ , then,

$$\begin{aligned}
\eta \|Q_{3,b}(RR^\top)^{-1}Q_{3,b}^\top\| \mathbf{I} &\preceq \eta \left( \frac{\eta}{\rho} \right)^2 (\kappa_2) \left( \frac{1}{\kappa_1} \right) \mathbf{I} \\
&= \left( \eta^3 \rho^{-2} \frac{\kappa_2}{\kappa_1} \right) \mathbf{I} \\
&= h_4(c) \mathbf{I}.
\end{aligned} \tag{80}$$

**By considering (74)–(80), it follows that (70b) holds.** Then we can move on and combine (70a) and (70b) to obtain the following:

$$\begin{aligned}
Q_1 - Q_3 Q_2^{-1} Q_3^\top &\succeq (2\eta c - \eta\ell)H - (h_1 + h_2(c) + h_3(c) + h_4) \mathbf{I} \\
&\succeq \left[ 2\eta\mu c - (\eta\mu\ell + h_1 + h_2(c) + h_3(c) + h_4) \right] \mathbf{I},
\end{aligned} \tag{81}$$

where we again have used  $\mu \preceq H$  from (43). Let

$$\Delta(c) := 2\eta\mu c - (\eta\mu\ell + h_1 + h_2(c) + h_3(c) + h_4), \tag{82}$$

then (81) is implied from  $Q_1 - Q_3 Q_2^{-1} Q_3^\top \succeq \Delta(c) \mathbf{I}$ . We now show that  $\Delta(c_o) > 0$  for the choice  $c = c_o$ , where  $c_o$  denotes the smallest admissible value satisfying (21d), i.e.,  $c_0 \geq 20\ell \left[ \max\left(\frac{\rho\kappa_2}{\mu}, \frac{\ell}{\mu}\right) \right]^2 \left[ \max\left(\frac{\eta}{\ell\rho}, \frac{\ell}{\mu}\right) \right]^2 \frac{\kappa_2}{\kappa_1}$ . To this end, define

$$q_\rho := \max\left(\frac{\rho\kappa_2}{\mu}, \frac{\ell}{\mu}\right), \tag{83a}$$

$$q_\eta := \max\left(\frac{\eta}{\ell\rho}, \frac{\ell}{\mu}\right), \tag{83b}$$

and set  $c = c_o$ , where we take equality in (21d), i.e.,

$$c_o := 20\ell q_\rho^2 q_\eta^2 \frac{\kappa_2}{\kappa_1}. \tag{84}$$

By construction, the following inequalities hold:

$$\rho\kappa_2 \leq q_\rho\mu, \quad \ell \leq q_\rho\mu, \quad \eta \leq q_\eta\ell\rho, \quad q_\rho \geq 1, \quad q_\eta \geq 1: \tag{85}$$

We note in particular that  $q_\rho \geq 1$  and  $q_\eta \geq 1$  due to the fact that  $\mu \leq \ell \Leftrightarrow 1 \leq \ell/\mu$  according to Proposition 2 and Assumption 4. Substituting (84) into  $2\eta\mu c$  yields

$$2\eta\mu c_o = 40\eta\mu\ell q_\rho^2 q_\eta^2 \frac{\kappa_2}{\kappa_1}. \tag{86}$$

**Next, we will produce a lower bound for  $\Delta(c_o)$  by finding bounds for each of its composing terms.** Note that since  $\kappa_2/\kappa_1 \geq 1$ , due to Assumption 5, then  $q_\rho^2 q_\eta^2 \frac{\kappa_2}{\kappa_1} \geq 1$ . As a consequence, (86) implies that

$$\eta\mu\ell \leq \frac{1}{40} (2\eta\mu c_o). \tag{87}$$

Next, recall that

$$h_1 = 2\eta^2\kappa_2 + \frac{\eta^2\kappa_1}{2}. \tag{88}$$

Since  $\kappa_1 \leq \kappa_2$  (by Assumption 5), it follows that

$$h_1 \leq \frac{5}{2}\eta^2\kappa_2. \tag{89}$$

Using  $\eta \leq q_\eta \ell \rho$  and  $\rho \kappa_2 \leq q_\rho \mu$  from (85), we further obtain that

$$h_1 \leq \frac{5}{2} \eta (q_\eta \ell \rho) \kappa_2 \leq \frac{5}{2} (\eta \mu \ell) q_\eta q_\rho. \quad (90)$$

From (86),  $\eta \mu \ell = \frac{1}{20} \frac{\eta \mu c_0}{q_\rho^2 q_\eta^2 \frac{\kappa_2}{\kappa_1}}$ . As noted earlier,  $q_\rho, q_\eta \geq 1$ . Also,  $\kappa_2/\kappa_1 \geq 1$  due to Assumption 5. Then, the following is implied from (90):

$$h_1 \leq \frac{1}{16} (2\eta \mu c_o). \quad (91)$$

For  $h_2(c)$ , recall that

$$h_2(c_o) = 2\eta \ell (\rho \kappa_2 + \frac{\eta \kappa_1}{2c_0}) + \eta (\rho \kappa_2 + \frac{\eta \kappa_1}{2c_0})^2. \quad (92)$$

Using  $c_o = 20\ell q_\rho^2 q_\eta^2 \frac{\kappa_2}{\kappa_1}$  from (84) and  $\rho \kappa_2 \leq q_\rho \mu$  from (85), we get from (92) that

$$h_2(c_o) \leq 2\eta \ell (q_\rho \mu + \frac{\eta \kappa_1^2}{40\ell q_\rho^2 q_\eta^2 \kappa_2}) + \eta (q_\rho \mu + \frac{\eta \kappa_1^2}{40\ell q_\rho^2 q_\eta^2 \kappa_2})^2,$$

Since  $q_\rho, q_\eta \geq 1$  (see (85)) and  $\kappa_2 \geq \kappa_1$  (see Assumption 5), it follows that

$$h_2(c_o) \leq 2\eta \ell (q_\rho \mu + \frac{\eta \kappa_1}{40\ell}) + \eta (q_\rho \mu + \frac{\eta \kappa_1}{40\ell})^2.$$

Given that  $\eta \leq q_\eta \ell \rho$  and  $q_\eta \geq 1$  (see (85)), the above expression implies that

$$h_2(c_o) \leq 2\eta \ell (q_\eta q_\rho \mu + \frac{q_\eta \ell \rho \kappa_1}{40\ell}) + \eta (q_\eta q_\rho \mu + \frac{q_\eta \ell \rho \kappa_1}{40\ell})^2.$$

Using again the facts that  $\kappa_2 \geq \kappa_1$  and  $\rho \kappa_2 \leq q_\rho \mu$ , we further get that

$$h_2(c_o) \leq 2\eta \ell (\frac{41q_\eta q_\rho \mu}{40}) + \eta (\frac{41q_\eta q_\rho \mu}{40})^2.$$

From (86),  $q_\rho q_\eta \mu = \frac{2\eta \mu c_0}{40\eta \mu \ell q_\rho q_\eta \frac{\kappa_1}{\kappa_2}}$ , then

$$\begin{aligned} h_2(c_o) &\leq 2\eta \ell (\frac{41q_\eta q_\rho \mu}{40}) (\frac{2\eta \mu c_o}{40\eta \mu \ell q_\rho^2 q_\eta^2 \frac{\kappa_2}{\kappa_1}}) + \eta (\frac{41q_\eta q_\rho \mu}{40})^2 (\frac{2\eta \mu c_o}{40\eta \mu \ell q_\rho^2 q_\eta^2 \frac{\kappa_2}{\kappa_1}}) \\ &= (2\eta \mu c_o) \frac{\kappa_1}{\kappa_2} \left( \frac{41}{800 q_\rho q_\eta} + \frac{1681 \mu}{64000 \ell} \right). \end{aligned}$$

Considering that  $q_\rho, q_\eta \geq 1$ , due to (85),  $\kappa_1/\kappa_2 \leq 1$ , due to Assumption 5, and  $\mu/\ell \leq 1$ , due to Proposition 2 and Assumption 4, we obtain the following inequality for  $h_2(c)$ :

$$h_2(c_o) \leq \frac{4961}{64000} (2\eta \mu c_o). \quad (93)$$

Now for  $h_3(c)$ , recall that

$$h_3(c) = \frac{2\eta^2}{\rho} \left( \ell + \rho \kappa_2 + \frac{\eta \kappa_1}{2c} \right) \frac{\kappa_2}{\kappa_1}. \quad (94)$$

Using  $\ell \leq q_\rho \mu$  and  $\rho \kappa_2 \leq q_\rho \mu$  from (85) and  $c = c_o = 20\ell q_\rho^2 q_\eta^2 \frac{\kappa_2}{\kappa_1}$  from (84), we obtain the following:

$$h_3(c_o) \leq \frac{2\eta^2}{\rho} \left( 2q_\rho \mu + \frac{\eta \kappa_1^2}{40\ell q_\rho^2 q_\eta^2 \kappa_2} \right) \frac{\kappa_2}{\kappa_1}.$$

Since  $q_\rho, q_\eta \geq 1$  (see (85)),  $\kappa_2 \geq \kappa_1$  (see Assumption 5), it further follows that

$$h_3(c_o) \leq \frac{2\eta^2}{\rho} \left( 2q_\rho \mu + \frac{\eta \kappa_1}{40\ell} \right) \frac{\kappa_2}{\kappa_1}.$$

From (85),  $\eta \leq q_\eta \ell \rho$  and  $q_\eta \geq 1$ . Then,

$$h_3(c_o) \leq \frac{2\eta^2}{\rho} \left( 2q_\eta q_\rho \mu + \frac{q_\eta \ell \rho \kappa_1}{40\ell} \right) \frac{\kappa_2}{\kappa_1}.$$

Using again the inequalities  $\kappa_2 \geq \kappa_1$  (see Assumption 5) and  $\rho\kappa_2 \leq q_\rho\mu$  (see (85)), leads to

$$h_3(c_o) \leq \frac{2\eta^2}{\rho} \left( \frac{81q_\eta q_\rho \mu}{40} \right) \frac{\kappa_2}{\kappa_1}.$$

Given that  $\eta \leq q_\eta \ell \rho$  (see (85)), and using  $q_\rho q_\eta \mu = \frac{2\eta\mu c_o}{40\eta\mu\ell q_\rho q_\eta \frac{\kappa_1}{\kappa_2}}$  from (86), then the following expression can be obtained:

$$h_3(c_o) \leq \frac{2\eta}{\rho} (q_\eta \ell \rho) \left( \frac{81q_\eta q_\rho \mu}{40} \right) \frac{\kappa_2}{\kappa_1} \frac{2\eta\mu c_o}{40\eta\mu\ell q_\rho^2 q_\eta^2 \frac{\kappa_2}{\kappa_1}} = \frac{81}{800q_\rho} (2\eta\mu c_o).$$

Since  $q_\rho \geq 1$  (see (85)), we can obtain a suitable upper bound for  $h_3(c)$  as follows:

$$h_3(c_o) \leq \frac{81}{800} (2\eta\mu c_o). \quad (95)$$

Finally, recall that

$$h_4 = \eta^3 \rho^{-2} \frac{\kappa_2}{\kappa_1}. \quad (96)$$

From (85), it holds that  $\frac{\eta}{\rho} \leq q_\eta \ell$ . Then,

$$h_4 \leq \eta q_\eta^2 \ell^2 \frac{\kappa_2}{\kappa_1}.$$

Through (86),  $\frac{2\eta\mu c_o}{40\eta\mu\ell q_\rho^2 q_\eta^2 \frac{\kappa_2}{\kappa_1}} = 1$ , then

$$h_4 \leq \eta q_\eta^2 \ell^2 \frac{\kappa_2}{\kappa_1} \left( \frac{2\eta\mu c_o}{40\eta\mu\ell q_\rho^2 q_\eta^2 \frac{\kappa_2}{\kappa_1}} \right),$$

which after simplification leads to

$$h_4 \leq \frac{\ell}{40\mu q_\rho^2} (2\eta\mu c_o).$$

Since from (85) it holds that  $\frac{\ell}{\mu} \leq q_\rho$  and  $q_\rho \geq 1$ , then

$$h_4 \leq \frac{1}{40} (2\eta\mu c_o). \quad (97)$$

Collecting the bounds (87), (91), (93), (95), and (97), we obtain that

$$\begin{aligned} \eta\mu\ell + h_1 + h_2(c_o) + h_3(c_o) + h_4 &\leq \left( \frac{1}{40} + \frac{1}{16} + \frac{4961}{64000} + \frac{81}{800} + \frac{1}{40} \right) (2\eta\mu c_o) \\ &= 0.291 (2\eta\mu c_o). \end{aligned} \quad (98)$$

**With (98) we can produce a lower bound for  $\Delta(c_o)$  as follows:**

$$\Delta(c_o) \geq (1 - 0.291) (2\eta\mu c_o) > 0. \quad (99)$$

Consequently, from (81),

$$Q_1 - Q_3 Q_2^{-1} Q_3^\top \succ 0. \quad (100)$$

Thus, the shifted Aug-PDGD is strictly passive with quadratic storage function  $S_c(\tilde{\theta}) = \tilde{\theta}^\top P_2 \tilde{\theta}$  and with respect to the input-output pair  $(\tilde{v}_{\text{pd}}, 2B_{\text{pd}}^\top P_2 \tilde{\theta})$ .  $\blacksquare$